UNIVERSITY OF CINCINNATI

May 25 1950

I hereby recommend that the thesis prepared under my supervision by William Licht, Jr.

entitled Studies of the Adsorption Wave in Beds of Granular Anhydrous Calcium Sulphate

be accepted as fulfilling this part of the requirements for the degree of Doctor of Philosophy

Approved by:

R. F. [illegible]

Ray O. McDuffie

E. F. Farnau

Hoke S. Greene

Form 668—G.S. and T.C.—500—5-45

STUDIES OF THE ADSORPTION WAVE IN BEDS OF GRANULAR ANHYDROUS CALCIUM SULPHATE

A dissertation submitted to the

Graduate School of Arts and Sciences
of the University of Cincinnati

in partial fulfillment of the
requirements for the degree of

DOCTOR OF PHILOSOPHY

William Licht, Jr.

Ch.E. University of Cincinnati 1937
M.S. University of Cincinnati 1939

Table of Contents

Table of Contents (continued)

List of Tables

List of Figures

Table of Symbols

A = cross-sectional area of bed container, normal to direction of flow.

a_p = surface area per particle.

a_v = surface area per unit volume of particles.

B = constant ratio of W to H^* for a linear static equilibrium adsorption isotherm.

B' = fB

b = a factor in the kinetic relationship for moisture pick-up. $= \frac{1}{rB}$, time^{-1}.

D_{A_m} = mean diffusivity of water in the carrier gas film.

D_I = internal diffusion coefficient.

d = a constant in the empirical equation for the mass transfer coefficient.

E = the function which is the exact solution of the basic differential equation.

F = the function which is the approximate solution of the basic differential equation.

f = ratio of W to W_s.

G = mass velocity of flow of dry air = Q/A

H = absolute humidity of air stream at any point and time.

H_g = absolute humidity corresponding to the back pressure created by moisture in the granule.

H^* = absolute humidity of air in equilibrium with moist surface of solid desiccant.

H_i^* = absolute humidity of air trapped in void spaces of bed at the beginning of run.

H_o = absolute humidity of air entering the bed.

H_z = absolute humidity of air leaving the bed.

I_o = Bessel function of the first kind of zero order and imaginary argument.

J_o = Bessel function of the first kind and zero order.

K_G = mass transfer coefficient, based upon absolute humidities.

k_G = mass transfer coefficient, based upon partial pressures.

K_s = shell diffusion coefficient.

M_G = molecular weight of carrier gas.

n = a constant in the empirical equation for the mass transfer coefficient.

P = total pressure of gas stream.

p = vapor pressure of water or ice.

$\mathcal{Q}$ = mass of dry air flowing per unit time.

R = radius of granule, outside surface.

r = resistance to moisture adsorption, units of time.

r_{MT} = resistance due to mass transfer.

r_{SD} = resistance due to surface diffusion.

r_{ID} = resistance due to internal diffusion.

S = a variable of integration.

T = generalized parameter, proportional to time = bt, dimensionless.

t = time elapsed from start of run.

Δt = time required for fluid to traverse the length of the bed.

v = a summation index.

W = average moisture content of granules, mass of water per unit mass of dry solid.

W_i = average moisture content of granules, at beginning of run.

W_o^* = moisture content of solids which would be in equilibrium with inlet air.

W_s = local moisture concentration at surface of solid granules.

X = generalized parameter proportional to length of bed = $\frac{\rho_B Z}{Gr}$, dimensionless.

x = any variable.

Y = $\sqrt{T} - \sqrt{X}$, using positive roots only.

y = $\sqrt{T} - \sqrt{S}$, a variable of integration.

Z = total length of bed.

z = distance from inlet end to any point in the bed.

Greek letters.

α = fraction of void volume in the bed.

ϕ = functional notation for the probability integral.

μ = viscosity of gas stream.

ρ_B = bulk density of bed, mass of solids per unit volume of container.

ρ_f = density of air film on surface of granule.

ρ_G = density of air-vapor moisture

ρ_p = density of dry desiccant particles.

ACKNOWLEDGEMENT

The author is very grateful to Professor R. S. Tour for his stimulating guidance and generous assistance in the capacity of thesis supervisor.

Mr. Cullen Mc. Cooper rendered an invaluable service with portions of the experimental work in the capacity of research assistant, and Dr. C. I. Lubin kindly assisted with certain mathematical questions.

Abstract

Theoretical and experimental contributions to the study of the behavior of beds of granular desiccants in removing moisture from a flowing gas stream are presented. A differential equation for the performance of such a bed is developed under various limiting assumptions regarding the mechanism of the process. Rigorous and approximate solutions to the equation, together with a method of testing experimental data for conformity to it, are developed. Critical analysis of previous contributions to this theory is undertaken.

The experimental work consists of further developments in the technique of measuring the performance of a bed, and of obtaining data showing the effect of the velocity of the air stream. A new apparatus for regeneration of desiccant *in situ* is presented. The method of using the Jury frost-point hygrometer to analyze the moisture content of an air stream is modified based upon the important discovery that sub-cooled water droplets may exist in this instrument at temperatures down to -40°F.

All of the valid experimental data available is subjected to analysis. Conformity with the differential equation is found only during the early part of the life of the bed. During this time, mass transfer seems to control the rate of moisture adsorption. For the latter

part of the bed life exhaustion becomes increasingly more rapid. This is attributed to an appreciable increase in the resistance to internal diffusion of water molecules through the granules as saturation is approached.

INTRODUCTION

The research carried out in this investigation was originally motivated by the practical problem of removing water vapor from large quantities of moist gases. During the recent war, the U. S. Army Air Force required a method of drying large amounts of compressed oxygen to be used in high-altitude flying operations. It was desired to remove moisture to the extent that no freezing or deposition of ice could occur when the gas was taken into the stratosphere and cooled to about -67°F. This corresponds to lowering the moisture content to the neighborhood of 10 parts per million at atmospheric pressure. A satisfactory solution to this drying problem was obtained by passing the gas through cannisters containing a specially treated material similar to granular anhydrous calcium sulphate. Provided that the initial moisture content of the gas, rate of flow of the gas, the particle size of the desiccant, and the dimensions of the bed contained in the cannister bore the proper relationship to one another, the special calcium sulphate removed the water vapor from the air stream to the desired extent. Anhydrous calcium sulphate, on the market under the trade name of Drierite, has been in common use as a drying agent for a variety of gases and liquids for some years.

It was considered desirable to undertake an investigation into the fundamental mechanism by which this desiccant operates in removing water vapor from gases in order to gain a more complete understanding of the relationships of this mode

of drying. Some preliminary work was carried out by Wheat (19), and an extensive study of some phases of the problem was made by Jury (11). The present study continues the investigation into some questions remaining unanswered by the previous work.

At the outset the problem was recognized as a special case of the general problem of the adsorption wave (13) which may be stated in the following terms. A stream of gas carrying a constituent which is to be removed (adsorbate) is passed through a fixed bed of granular solid at a steady rate. The solid material (adsorbent) is capable of adsorbing, or in some manner taking up the removable constituent but not the carrier gas. As a result, the carrier gas stream issues from the bed with a much reduced concentration of adsorbate. At the beginning of the operation this outlet concentration may be very low, but as the capacity of the bed for adsorbate becomes exhausted, this concentration will gradually rise. Ultimately, if the bed is carried to complete exhaustion, it will attain the same value as that of the entering gas. Assuming the concentration of adsorbate to be uniform across the diameter of the bed at any point, the adsorption wave may be defined as a functional relationship which gives H, the concentration of adsorbate in the gas stream, as a function of z, the distance through the bed from the inlet end, and t, the time elapsed since the flow was started. The general problem is to find this functional relationship and to elucidate the effect of

some pertinent variables upon it. Obviously, we are dealing here with an unsteady state problem. The concentration may be conveniently expressed as the ratio of mass of adsorbate vapor to mass of carrier gas, i.e., the "absolute humidity" H. Thus it is desired to find in general

$$H = H\ (z,\ t)$$

A special point of particular interest is, of course, the concentration H_z in the stream issuing from the outlet end of the bed. This will be determined by the same functional expression:

$$H_Z = H\ (Z,\ t)$$

The exact nature of the adsorption wave will depend upon the specific vapor-adsorbent system as well as upon certain general principles applicable to this operation with any system, For the particular system water vapor-anhydrous calcium sulphate herein studied, development of the functional relationship requires a knowledge of the exact manner by which water is removed from the air and taken up by the solid. It is also very desirable that we be able to describe in mathematical terms the rate at which water vapor moves from the air stream up to the surface and into the interior of the granules. The general term adsorption has been used here to denote this process without any specific technical connotation as to the exact manner in which it occurs.

The problem may be attacked from the theoretical standpoint by considering either an infinitesimal element of bed length or the bed as a whole and setting up a partial

differential equation based upon a material balance over the element or the entire bed. To obtain a solution to this equation, it is necessary to assume some definite relationship for the rate of water pickup by the granules. Various solutions may be obtained depending upon the relationship assumed. Klotz (13) has given an excellent review of many of these, and Jury (11) has developed others which will be described further in detail. These solutions have usually been presented in terms of the outlet concentration ratio H_{Z/H_O}, where H_O is the absolute humidity of the inlet stream.

Experimentally, the problem may be attacked either in a purely empirical manner, or in a way such as to verify, supplement, or modify the theoretical approach. In either case, all workers thus far have employed the same procedure, namely of measuring H_Z as a function of time, for a fixed set of operating conditions including bed length Z, inlet concentration H_O, bed diameter, desiccant granule size, air flow rate, temperature and pressure. The empirical approach would consist of accumulating numerous graphs of H_Z vs. t for an assortment of combinations of the other variables. While laborious, this may be desirable or necessary in certain applications. The alternative is to run selective experiments designed to establish which particular solution of the partial differential equation is correct and to establish the value of certain constants appearing therein, and then to use that solution for design purposes in practical application. The latter method

is probably the best whenever it can be employed. The experimental work carried out in this investigation has been of this type.

There are two important adjuncts to such studies. One is knowledge of the chemical and physical nature of the adsorbent and vapor. Particularly, the static adsorption equilibrium isotherms are needed. These have been partially determined by Jury (11) for the water-calcium sulphate system. The other auxiliary problem is the development of a method for analyzing the gas stream in order to get instantaneous values of H_o and H_z. For use in conjunction with any system when water vapor is the adsorbate, Jury designed and constructed an electronic frost-point hygrometer (11) which has been used in a modified way throughout this work.

The discussion which follows has been divided into two principal portions: contributions to the theoretical approach and contributions to the experimental approach.

Theoretical Approach

Previous developments with theory of the adsorption wave as it applies to a bed of desiccant have been presented by Marshall and Pigford (15), Hougen and Marshall (8) and Jury (11). Three distinct steps are involved in the theory: first, the development of a preliminary partial differential equation based upon a material balance over the bed; second, insertion into this equation of an expression for the rate of moisture pick-up by the granules based upon the assumption of a fixed rate-controlling resistance, this resistance dependent on the mechanism; and third, the solution of the resulting differential equation in conformity with certain boundary conditions. We shall develop the theory mathematically as far as possible, including a critical review of previous contributions as well as necessary modifications and extensions, and a method of subjecting it to experimental testing.

The Material Balance:

The material balance is usually developed for an infinitesimal length of bed. We shall present an alternative development based upon the entire bed. In time, t, elapsed after the inlet air stream is turned on, the total amount of moisture which enters the bed will be equal to H_oQt, where Q is the mass of air (dry basis) entering per unit time. This moisture must be accounted for in one of three ways:

1) moisture in the outlet air stream,

2) moisture taken up by the solids,

3) moisture in the air left trapped in the void spaces of the bed.

In computing item (1), any moisture in the air trapped in the void spaces at the beginning of the run must be deducted, as this will merely be swept out in the first portion of air leaving the bed. This deduction, as well as item 3, will be negligibly small and we shall neglect both in developing and using the differential equation. However, in order to clear up some confusion in the literature on this point, we shall later show how these items may be calculated and what they lead to when included.

Neglecting the deduction from item (1), and item (3), the terms of the material balance may be written:

$$Q\int_o^t H_z dt = \text{moisture in the outlet air stream.}$$

$$\rho_B A\int_o^Z (W-W_i)dz = \text{total moisture taken up by the solids}$$

Here, in addition to the other symbols previously defined:

A = cross sectional area of the bed, normal to direction of flow.

ρ_B = bulk density of solids, mass of solids per unit volume of bed container; assumed constant.

W = moisture content of solids, at any time and location in the bed, mass of moisture per unit mass of desiccant (dry basis); assumed uniform over any cross-section of bed; in functional notation $W = W(z, t)$.

W_i = moisture content of solids before run started; assumed constant throughout the bed and in equilibrium with the air trapped in the void spaces of the bed.

For the material balance then:

$$H_o Qt = Q\int_o^t H_Z dt + \rho_B A \int_o^Z (W-W_i)dz \quad - - - - - - - - (1)$$

Dividing through by A and letting $G = \frac{Q}{A}$, the mass velocity of air flow based upon the cross-sectional area of the bed container,

$$H_o Gt = G\int_o^t H_Z dt + \rho_B \int_o^Z (W-W_i)dz$$

Differentiating, first with respect to t; at constant Z:

$$H_o G = GH_Z + \rho_B \int_o^Z \frac{\partial W}{\partial t} dz$$

and then with respect to Z; at constant t:

$$\frac{\partial H_Z}{\partial Z} + \frac{\rho_B}{G} \frac{\partial W_Z}{\partial t} = 0$$

This is the preliminary differential equation referred to above. Obviously, the same equation will hold for any point in the bed as the endpoint so that the subscripts Z are not needed:

$$\frac{\partial H}{\partial z} + \frac{\rho_B}{G} \frac{\partial W}{\partial t} = 0 \quad - - - - - - - - - - - - - - - (2)$$

If the items neglected above are to be included, they will appear as follows:

$QH_i^* \Delta t$ = moisture trapped in void spaces at the beginning of the run.

$\alpha A \rho_G \int_o^Z Hdz$ = moisture trapped in void spaces at the end of the run.

where α = fraction void space in the bed; assumed constant

ρ_G = density of the air-water mixture at any point; assumed constant

H_i^* = absolute humidity of air trapped in void spaces at beginning of the run; assumed to be in equilibrium with W_i, the initial moisture content of the solids.

Δt = time required for the air stream to traverse the length of the bed.

Inclusion of these terms in the material balance gives:

$$H_o Qt = Q\int_o^t H_z dt - QH_i^* \Delta t + \rho_B A\int_o^Z (W-W_i)dz + \alpha A\rho_G\int_o^Z Hdz \quad ---(3)$$

When this equation is treated in the same manner as (1), i.e., dividing through by A and differentiating with respect to t and Z in turn, we obtain finally:

$$\frac{\partial H}{\partial z} + \frac{\rho_B}{G}\frac{\partial W}{\partial t} + \frac{\alpha\rho_G}{G}\frac{\partial H}{\partial t} = 0 \quad ---------(4)$$

By comparison with equation (2) it is seen that an additional term involving $\frac{\partial H}{\partial t}$ arises when the items dealing with the moisture in the air trapped in the void spaces of the bed are included. The real reason, then, for the appearance (or lack of it) of such a term in the basic differential equation is clearly shown. The presentation of the development of this equation by Jury does not make the point clear.

Returning to equation (2), then, and using it for further development, it becomes evident that the next step requires an expression relating W and H so that the number of variables in the equation may be reduced from four (H, W, z, t) to three, either H, z, t or W, z, t. This must be done by considering the kinetics of the adsorption process in order to get another expression for $\frac{\partial W}{\partial t}$, the local rate of

moisture pickup. It is here that a knowledge of the physical and chemical properties of the system to be dealt with must be brought in.

Kinetic Relationships:

The rate at which moisture is taken up by a granule is determined primarily by the resistance the water molecules encounter in moving from the gas phase into and through the solid phase. There can only be two basic locations of resistance, either external to the solid, or within the solid. The resistance external to the solid is due to the viscous film of gas on the surface of the granules through which the water molecules must pass by diffusion, a process referred to as "mass transfer". The resistance within the granule may be of two types: either at the surface (resistance to water molecules entering the pores of the solid) or within the body of the granule (resistance to internal diffusion of water molecules through the space lattice of the desiccant). We may then consider three types of resistance: extra-granular (mass transfer), surface granular, and intra-granular (internal diffusion).

We shall examine the known facts about each of these processes in turn, and see how they may be adapted to the problem at hand. It will be shown that all three cases may be generalized into the same type of kinetic relationship of the form:

$$\frac{\partial W}{\partial t} = \frac{\text{driving force}}{\text{resistance}} = \frac{H - W/B}{r} \qquad \text{- - - - - - -(5)}$$

wherein the "driving force" is always equal to $(H - \frac{W}{B})$ and the "resistance" r will be expressed in terms of the appropriate factors or coefficients entering into each case. This generalization will prove to be very convenient in developing the differential equation of the bed.

Kinetic Relationships: Mass Transfer:

The kinetic relationship in the case of mass transfer has been presented by Hougen and Marshall (8). It is based upon the assumption that the rate of moisture diffusion across the gas film is proportional to the difference between the prevailing value of H, and the value H^* which would represent equilibrium with the moist surface of the solid. The relationship given for a dilute gas-vapor mixture at ordinary pressure is:

$$\text{rate of mass transfer} = \frac{K_G a_v}{\rho_B} (H-H^*) \quad - - - - -(6)$$

or an alternative expression

$$\text{rate of mass transfer} = \frac{k_G M_G P_G a_v}{\rho_B} (H-H^*) \quad - - -(6a)$$

wherein: k_G = mass transfer coefficient, on basis of partial pressures.

$K_G = k_G M_G P_G$ = mass transfer coefficient, on basis of absolute humidities.

M_G = molecular weight of gas.

P_G = total pressure of gas vapor mixture surrounding the granules.

a_v = specific area of particle surface, area per unit volume of particles.

It is to be noted that these equations may be expressed in

a standard kinetic form:

$$\text{rate} = \frac{\text{driving force}}{\text{resistance}}$$

wherein the driving force = $H-H^*$

and the resistance = $\frac{\rho_B}{K_G a_v} = \frac{\rho_B}{k_G M_G P_G a_v}$

In addition to the factors ρ_B, M_G, P_G, a_v, and $(H-H^*)$ which appear explicitly, the rate will be influenced by other variables which affect k_G (or K_G) such as the velocity of gas flow over the surface, the nature (viscous or turbulent) of the gas flow, viscosity and density of the gas, and size and shape of the particles. Gamson, Thodos, Wilke and Hougen (5, 23) have obtained experimental data which indicate that K_G is related to the other variables according to:

$$\frac{K_G}{G}\left(\frac{\mu_f}{\rho_f D_{A_m}}\right)^{2/3} = d\left(\frac{\sqrt{a_p}\,G}{\mu}\right)^{-n} \qquad \text{-------(7)}$$

wherein μ = viscosity of gas stream

μ_f = viscosity of gas film

ρ_f = density of gas film

D_{A_m} = mean diffusivity through gas film

a_p = surface area per granule

d, n = constants, value depending upon range of $\frac{\sqrt{a_p}G}{\mu}$

For $\frac{\sqrt{a_p}G}{\mu} < 620$ d = 2.44; n = 0.51

$\frac{\sqrt{a_p}G}{\mu} > 620$ d = 1.25; n = 0.41

The group $\frac{\sqrt{a_p}G}{\mu}$ is seen to be a modified Reynold's number

by means of which the data for k_G were correlated. However, the value of 620 has no particular significance; it was arbitrarily selected because it seemed necessary to use two sets of constants to best fit the data. Actually, all of the data correlated by these expressions corresponds to turbulent flow, well above the upper limit of the viscous flow range which is placed at a value of about 40. For the viscous range n = 2.

It is of interest to note here that, in particular

$$K_G \propto d\, G^{1-n}$$

and

$$K_G \propto \frac{d}{a_p^{n/2}} \propto \frac{d}{(R^2)^{n/2}} = \frac{d}{R^n} \qquad \text{------(8)}$$

when R is a characteristic linear dimension, as the radius, of a granule.

Very little use can be made of equation (6) unless it is possible to relate H^* to the moisture content of the granule. It is the moisture concentration on the surface of the granule which really determines H^*, but the relation which this bears to the total moisture picked up by the granules at any time may not be known. To use equation (6) in the customary way, we are really forced to assume that the moisture picked up is uniformly distributed throughout the granules, i.e., that the rate of diffusion inside the solid is very rapid in comparison with the rate of mass transfer. Then we may use the experimentally determined static equilibrium adsorption isotherm to relate

W and H^*. For many systems, the linear relationship

$$W = BH^* \qquad \text{- - - - - - - - - - - - - - - - - -(9)}$$

holds, wherein B is a constant for a given temperature and pressure on the system. Jury (11) found by experimental measurements of the static adsorption equilibrium that such a relationship was satisfactory for the anhydrous calcium sulphate system, provided W was below about 6.0.

As the static equilibrium isotherm is determined the term W always refers to the total moisture content divided by the total weight of the dry solid, i.e., the average total moisture concentration. In these static experiments, this moisture is uniformly distributed throughout the solid. Obviously, the relationship cannot then be applied to any case where the moisture distribution is non-uniform, such as arises in a dynamic experiment when the rate of internal diffusion is relatively slow. If the relationship is used in such a case, B cannot be expected to be constant at the value obtained from the static experiments. Let W_s be the surface moisture concentration. Then if (9) applies for static equilibrium and if the moisture were uniformly distributed throughout the granule

$$W = W_s = BH^*$$

But when $W \neq W_s$, suppose $W = fW_s$ where $f < 1$ for a drying operation. Then

$$W = fW_s = fB\,H^*$$

or $W = B'H^*$

Now only if f is constant, i.e. the surface moisture concentration bears a constant ratio to the average moisture concentration at all times, will B' be constant and even then B' must be less than B. It seems very unlikely that a constant f would ever occur, for at the beginning of a run W_s would be high while the moisture content in the interior would be very small and at the end when the granule is nearly saturated, W_s would be very nearly equal to W. Consequently, f would be small at the beginning and rise to approach 1 at the end of the run.

Assuming that there is relatively rapid internal diffusion, consequently, uniform moisture distribution within the granules, we may combine (6) and (9) to obtain an expression for $\frac{\partial W}{\partial t}$ which now is equal to the rate of mass transfer:

$$\frac{\partial W}{\partial t} = \frac{K_G a_v}{B} (H - \frac{W}{B}) = \frac{1}{r_{MT}} (H - \frac{W}{B}) \text{ - - - - - - - - -} (10).$$

This may be used with equation (2) whenever circumstances warrent. In so doing, it would be assumed that K_G and B are constant as the adsorption continues, i.e., that we have a constant resistance to mass transfer throughout any one run. This resistance, due to mass transfer, would obviously be $r_{MT} = \frac{B}{K_G a_v}$, so that equation (10) is of the general form of equation (5).

Equation (10) has been offered by Hougen and Marshall, and by Jury as a kinetic relationship for the mass

transfer rate without noting that it really involves assuming an infinite rate of internal diffusion. It cannot be expected to apply to the mass transfer which occurs in any bed where internal diffusion is a relatively slow process.

It is not likely that mass transfer alone can be the controlling factor throughout the entire life of any bed which is run to saturation. During the latter part of such a run, the internal resistance to moisture movement must increase considerably and probably becomes an important factor in controlling the overall rate of adsorption. Thus, any differential equation based upon (10) would not be likely to apply to the entire course of such a run, but only to the first part of it. If it were found to apply to experimental data, it would mean that mass transfer offered the dominating resistance to adsorption and that internal resistances were negligible.

For use in developing the differential equation of the bed, it will be seen later that the equation for $\frac{\partial^2 W}{\partial t^2}$ is needed. From (10) this will be:

$$\frac{\partial^2 W}{\partial t^2} = \frac{K_G a_v}{B} \frac{\partial H}{\partial t} - \frac{K_G a_v}{B^B} \frac{\partial W}{\partial t} \qquad \text{- - - - - -(11)}$$

or

$$\frac{\partial^2 W}{\partial t^2} = \frac{1}{r_{MT}} \frac{\partial H}{\partial T} - \frac{1}{r_{MT} B} \frac{\partial W}{\partial t}$$

The mathematical form of this is of interest for comparisnn

with other expressions to be developed.

Kinetic Relationships: Internal Processes

We shall consider first the case of internal diffusion and then the case of surface resistance.

To develop the kinetic relationship applicable to the case of internal diffusion, we may follow the work of Wicke (21, 22). He assumed a spherical granule of radius R having initially a uniform moisture concentration throughout and in equilibrium with the surrounding air. He then solved the basic partial differential equation of diffusion subject to the boundary condition that the surface of the granule is always in equilibrium with the surrounding air of continually changing humidity, and assuming that the relationship $W_S = BH$ applies. For the total moisture content at any time, he obtained:

$$W = BH - \frac{6B}{\pi^2} \sum_{v=1}^{\infty} \frac{1}{v^2} \int_0^t e^{-v^2 \frac{\pi^2 D_I}{R^2} (t-S)} \frac{\partial H}{\partial S} dS \quad ---(12)$$

In this expression D_I is called the internal diffusion coefficient which is supposed to be constant, depending only upon the nature of the lattice structure and of the diffusing molecules, as well as the temperature. However, it may well be that as the lattice becomes filled with water molecules, the value of this coefficient decreases, resistance to internal diffusion becoming larger. Upon differentiating (12) with respect to t, the kinetic relationship is

obtained:

$$\frac{\partial W}{\partial t} = \frac{6BD_I}{R^2} \sum_{v=1}^{\infty} \int_0^t e^{-v^2 \frac{\pi^2 D_I}{R^2} (t-S)} \frac{\partial H}{\partial S} dS \quad - - - - - (13)$$

This expression, involving as it does an infinite series, is rather too complicated to be of much practical use. However, a simplified approximation may be obtained to both (12) and (13) by using only the first term of each of these series. Thus

$$W \approx BH - \frac{6B}{\pi^2} \int_0^t e^{-\frac{\pi^2 D_I}{R^2} (t-S)} \frac{\partial H}{\partial S} dS$$

and

$$\frac{\partial W}{\partial t} \approx \frac{6BD_I}{R^2} \int_0^t e^{-\frac{\pi^2 D_I}{R^2} (t-S)} \frac{\partial H}{\partial S} dS$$

From this it is evident that when only the first term is considered in each series:

$$\frac{\partial W}{\partial t} = \frac{\pi^2 D_I}{R^2} (BH - W) = \frac{\pi^2 D_I B}{R^2} \left(H - \frac{W}{B}\right) - - - (15)$$

which is of precisely the same general form of equation (10) for mass transfer; the only difference lies in the nature of the resistance factor. Here the resistance to internal diffusion is $r_{ID} = \frac{R^2}{\pi^2 D_I B}$, so that

$$\frac{\partial W}{\partial t} = \frac{H - W/B}{r_{ID}}$$

The resistance r_{ID} will be constant so long as D_I is constant;

if D_I decreases as the bed approaches saturation, then r_{ID} will increase. The second derivative, required later, will be:

$$\left.\begin{aligned} \frac{\partial^2 W}{\partial t^2} &= \frac{\pi^2 D_I B}{R^2}\ \frac{\partial H}{\partial t} - \frac{\pi^2 D_I}{R^2}\ \frac{\partial W}{\partial t} \\ \text{or}\qquad \frac{\partial^2 W}{\partial t^2} &= \frac{1}{r_{ID}}\ \frac{\partial H}{\partial t} - \frac{1}{r_{ID} B}\ \frac{\partial W}{\partial t} \end{aligned}\right\} \text{-----(16)}$$

It is to be emphasized that in order to obtain equation (15), it is necessary to assume an infinite rate of mass transfer existing around the granule surface so that W_s may be taken to be always in equilibrium with H. Thus, equations (10) and (15) are mutually exclusive relationships; that is, if one applies, the other cannot because they are based upon assumptions which are exactly opposite. This fact has not been pointed out previously.

To develop a kinetic relationship for the surface-granular type of resistance, we may assume that resistance due to mass transfer and to internal diffusion are each negilgible. Then the surface moisture is in equilibrium with the air stream, and the bulk of the granules has a uniform moisture concentration. The rate of adsorption is then proportional to the difference between W_s and W. Jury has presented an equation for such a case, which he called "shell diffusion,"

$$\frac{\partial W}{\partial t} = K_s a_v\ (W_s - W)$$

which may be modified to accord with the previous presentations

above:

$$\left.\begin{aligned} &\frac{\partial W}{\partial t} = K_s a_v (BH - W) = K_s a_v B\left(H - \frac{W}{B}\right) \\ \text{or}\quad &\frac{\partial W}{\partial t} = \frac{H - W/B}{r_{SD}} \quad \text{where } r_{SD} = \frac{1}{K_s a_v B} \end{aligned}\right\} \quad - - -(17)$$

where K_s = shell diffusion coefficient

a_v = surface area per unit volume of particles.

The value of K_s will depend upon surface adsorption phenomena, preliminary treatment of surface, etc. It will be independent of properties or velocity of the gas stream. For any one run, it will be constant, and the resistance r_{ID} will be constant.

Equation (17) is seen to be of the same form as both (10) and (15). However, the assumptions upon which it is based make it mutually exclusive with these expressions. We thus have an individual expression for each case, but the form of all these rate equations is the same.

Kinetic Relationships Generalized:

It is clear from the above sections that we may generalize the entire treatment of these kinetic relationships in the following way. Take the rate of adsorption $\frac{\partial W}{\partial t}$ to be proportional to a driving force $(H - H_g)$ which is the difference between the humidity H of the air stream and a "back pressure humidity" H_g due to the moisture in the granule. This driving force is opposed by a resistance

r, so that

$$\frac{\partial W}{\partial t} = \frac{H - Hg}{r}$$

The "back pressure humidity" must be related to the average moisture content W of the granules. The relationship is $Hg = \frac{W}{B}$ in all three cases, the same relationship as for the static equilibrium adsorption isotherm. The resistance term r depends upon the specific nature of the resistance to be considered, but for all three cases, the basic differential kinetic relationship is

$$\left.\begin{aligned} \frac{\partial W}{\partial t} &= \frac{1}{r} H - \frac{1}{rB} W \\ \text{and} \qquad \frac{\partial^2 W}{\partial t^2} &= \frac{1}{r}\frac{\partial H}{\partial t} - \frac{1}{rB}\frac{\partial W}{\partial t} \end{aligned}\right\} \text{- - - - - -(18)}$$

If more than one resistance is significant, the term r will represent the total resistance which is the sum of the contributions of each individual type of resistance. If the magnitude of the individual resistances does not change during a run, this total will be constant also; if the proportion of each resistance changes in any way r will vary. But for the case of a constant total, combined resistance, the same differential relationship will hold as for any single type of resistance.

The only type of resistance which could vary during a run under the general conditions maintained in the work would be the internal diffusion. In the event that a more crowded space lattice would result in a reduced D_I, this

resistance r_{ID} would increase. If r_{ID} became appreciable in comparison with r_{MT} or r_{SD}, then near the end of the run the bed would exhaust more rapidly than would be anticipated from the rate of exhaustion during the first part of the run. The curve of log H_z/H_o vs. t would deviate upwards from the values to be expected by extending the initial portion of the curve. In such a case, the kinetic relationship (18) above would not have a constant r and the differential equation developed from it would become more complex; for then r would be some function of t (or W), and the value of $\frac{\partial^2 W}{\partial t^2}$ would be more complex:

$$\frac{\partial^2 W}{\partial t^2} = \frac{1}{r}\frac{\partial H}{\partial t} - \frac{H}{r^2}\frac{\partial r}{\partial t} - \frac{1}{rB}\frac{\partial W}{\partial t} + \frac{1}{r^2 B}\frac{\partial r}{\partial t}$$

No attempt has been made to treat equations of this kind; they would result, if soluble at all, in functions which are too complicated to be of practical value.

The Differential Equations:

To develop a final differential equation which applies to a bed, it is necessary only to combine the material balance (2) with the appropriate kinetic relationship (10), (15) or (17) in the following way. From (2) by differentiation:

$$\frac{\partial^2 H}{\partial z \partial t} = -\frac{\rho_B}{G}\frac{\partial^2 W}{\partial t^2} \qquad \text{- - - - - - -(19)}$$

From any of the kinetic relationships, an equation of the

form of (18) is obtained:

$$\frac{\partial^2 W}{\partial t^2} = \frac{1}{r}\frac{\partial H}{\partial t} - \frac{1}{rB}\frac{\partial W}{\partial t}$$

Thus (19) becomes:

$$\frac{\partial^2 H}{\partial z \partial t} = -\frac{\rho_B}{Gr}\frac{\partial H}{\partial t} + \frac{\rho_B}{GrB}\frac{\partial W}{\partial t} \qquad \text{- - - - - -(20)}$$

But from (2) also: $\frac{\rho_B}{G}\frac{\partial W}{\partial t} = -\frac{\partial H}{\partial z}$, so that (20) becomes:

$$\frac{\partial^2 H}{\partial z \partial t} + \frac{\rho_B}{Gr}\frac{\partial H}{\partial t} + \frac{1}{rB}\frac{\partial H}{\partial z} = 0 \qquad \text{- - - - - -(21)}$$

Now if for any one run r, B, ρ_B, and G are constant, we may let

$$X = \frac{\rho_B}{Gr} z$$

and

$$T = \frac{1}{rB} t = bt$$

whereupon, by substitution (21) becomes:

$$\frac{\partial^2 H}{\partial X \partial T} + \frac{\partial H}{\partial T} + \frac{\partial H}{\partial X} = 0 \qquad \text{- - - - - - - - -(22)}$$

This is the basic differential equation of the bed in its simplest mathematical form. It is to be noted that each of the individual kinetic relationships leads to this same equation. Further, a case of combined resistance which could be represented by (18) with r and B constant, would also lead to (22). If r and B were not constant in (18) but varied with W or T in some manner, a more complex differential equation would result.

A differential equation for W may also be developed

for those cases where we may take

$$\frac{\partial W}{\partial t} = \frac{1}{r} H - \frac{1}{rB} W \qquad \text{- - - - - - - -(23)}$$

with r and B constant. Differentiating again with respect to z

$$\frac{\partial^2 W}{\partial z \partial t} = \frac{1}{r}\frac{\partial H}{\partial z} - \frac{1}{rB}\frac{\partial W}{\partial z}$$

and replacing $\frac{\partial H}{\partial z}$ by (2):

$$\frac{\partial^2 W}{\partial z \partial t} = -\frac{\rho_B}{Gr}\frac{\partial W}{\partial t} - \frac{1}{rB}\frac{\partial W}{\partial z}$$

Again letting $X = \frac{B}{Gr} z$, and $T = \frac{1}{rB} t = b\,t$, we would have

$$\frac{\partial^2 W}{\partial X \partial T} + \frac{\partial W}{\partial T} + \frac{\partial W}{\partial X} = 0 \qquad \text{- - - - - - - - - - -(24)}$$

which is identically the same differential equation as (22) for H and will apply under the same conditions.

Solution of the Differential Equations:

Solutions to (22) and (24) based upon the boundary conditions that

H = Ho when X = 0 for all values of T and

W = W_i when T = 0 for all values of X

have been presented by Marshall and Pigford (15) as follows:

$$\frac{H - H_i^*}{H_o - H_i^*} = 1 - e^{-T}\int_o^X e^{-S} I_o(2\sqrt{XS})\, dS \qquad \text{- - - - - -(25)}$$

$$\frac{W - W_i}{W_o^* - W_i} = e^{-X}\int_o^T e^{-S} I_o(2\sqrt{XS})\, dS \qquad \text{- - - - - - - - -(26)}$$

where S = variable of integration

I_o = the functional notation for Bessel's function of order zero and imaginary argument, i.e., $I_o(x) = J_o(ix)$ where $i = \sqrt{-1}$.

J_o = Bessel's function of the first kind and zero order.

W_o^* = BH_o, moisture content of solids which would be in equilibrium with inlet air stream of humidity H_o.

The boundary conditions are easily verified since $I_o(0) = 1$. Further, equation (25) gives at $T = 0$,

$$\frac{H - H_i^*}{H_o - H_i^*} = e^{-X} \quad \text{for all values of } X \quad ----(27).$$

In case the bed is very dry at the outset, both W_i and H_i^* may be negligible and the ratios on the left side of (25) and (26) would become simply H/H_o and W/W_o respectively.

Computations with these solutions are complicated and inconvenient. For this reason, the solutions have been presented in a graphical form which is called a Schumann-Furnas chart. Such charts are available in a number of places, but perhaps the best copy is to be found in "Chemical Process Principles Charts" by Hougen and Watson (9). Values of the functions on the right hand side of (25) and (16) are plotted against $T = bt$ for a constant X; a family of curves covering a series of values of X are presented. These charts suffer from the serious disadvantage that a very laborious trial and error procedure is necessary in order to test experimental data against them when values of b and X are unknown. For this reason, a simplified approximate solution has been developed below

which may be readily used to test experimental data for conformity to the differential equation. The chart as published, is presented only in terms of a solution dealing with mass transfer. We have seen above, however, that the other kinetic relationships will also lead to the same differential equation. Hence, the chart is applicable to these other cases as well.

Jury presented a solution to (22) in a somewhat different form, which also assumed r and B to be constant, H_i^* and W_i to be zero, and was stated to fit boundary conditions such that

$H = H_o$ where $X = 0$ for all values of T

$H = 0$ where $T = 0$ for any value of X.

This solution is

$$\frac{H}{H_o} = 1 + e^{-T-X}I_o(2\sqrt{XT}) - e^{-X}\int_T^\infty e^{-S}I_o(2\sqrt{XS})dS \quad - - -(28)$$

It is easily shown that it fits the first boundary condition, but for the second

$$\frac{H}{H_o} = 1 + e^{-X} - e^{-X}\int_o^\infty e^{-S}I_o(2\sqrt{XS})dS \quad - - - -(29)$$

The integral in (29) has been evaluated by the author as e^X, based upon the general integral given by Frank and von Mises (4), as

$$\int_o^\infty e^{-p^2x^2}J_o(ax)xdx = \frac{1}{2p^2}e^{-\frac{a^2}{4p^2}} \qquad p \neq 0.$$

Here $a = 2i\sqrt{X}$

$p = 1$

$x = \sqrt{S}$

$J_o(ix) = I_o(x)$

Hence, from (29) with e^X for the integral,

$$H/H_o = 1 + e^{-X} - e^{-X} e^{X} = e^{-X} \quad - - -(30)$$

which is the same as (27) provided $H_1^* = 0$. Thus, the statement of the second boundary condition as given by Jury is not correct. Since Jury's solution is more complicated, based upon more restricted conditions, and yet actually conforms to the same boundary conditions as Marshall and Pigford's, we will use the latter.

The Approximate Solution:

Jury outlined a method of simplifying his solution which is worthy of note because it may be adapted to Marshall and Pigford's solution as well. This consists of replacing the Bessel function I_o by the asymptotic expansion

$$I_o(x) \rightarrow \frac{e^x}{(2\pi x)}1/2 \text{ as } x \rightarrow \infty$$

and assuming that $\left(\frac{S}{X}\right)^{1/4} \approx 1$

in the integral which results. This finally leads to an expression for

$$\left.\begin{aligned} \frac{H}{H_o} &= 1/2\left[1 + \phi(Y)\right] \\ \text{where} \quad \phi(Y) &= \frac{2}{\sqrt{\pi}}\int_o^Y e^{-y^2}\,dy \end{aligned}\right\} - - - -(31)$$

and $(Y = \sqrt{T} - \sqrt{X} = \sqrt{bt} - \sqrt{X})$ only positive roots being used.

ϕ (Y) is the well known probability function for which tables are available, as in Lange's "Handbook of Chemistry" (14). As will be shown later, this approximate solution can be very well adapted to the testing of experimental data. Jury did not investigate just how closely his approximation (31) represented the rigorous solution (28).

In order to develop a simplified representation of Marshall and Pigford's solution, we proceed from equation (25):

$$\frac{H - H_i^*}{H_o - H_i^*} = 1 - e^{-T}\int_{\infty}^{X} e^{-S} I_o(2\sqrt{ST})dS = E$$

First break the integral into two parts:

$$\frac{H - H_i^*}{H_o - H_i^*} = 1 - e^{-T}\int_{o}^{\infty} e^{-S} I_o(2\sqrt{ST})dS + e^{-T}\int_{x}^{\infty} e^{-S} I_o(2\sqrt{ST})dS = E$$

Now the first integral is similar to that in equation (29) and has the value e^T. The equation, therefore, reduces to:

$$\frac{H - H_i^*}{H_o - H_i^*} = e^{-T}\int_{x}^{\infty} e^{-S} I_o(2\sqrt{ST})\, dS = E$$

Following Jury's method, replace $I_o(2\sqrt{ST})$ by the asymptotic expansion

$$\frac{2\sqrt{ST}}{(4\pi\sqrt{ST})}1/2, \text{ then}$$

$$\frac{H - H_i^*}{H_o - H_i^*} = \frac{1}{2\sqrt{\pi}}\int_{x}^{\infty} \frac{e^{-T + 2\sqrt{ST} - S}}{(ST)^{1/4}} dS$$

But $-\sqrt{T} + 2\sqrt{ST} - \sqrt{S} = -(\sqrt{T} - \sqrt{S})^{1/2}$, and letting $y = \sqrt{T} - \sqrt{S}$, then

$$\frac{H - H_i^*}{H_o - H_i^*} = \frac{1}{2\sqrt{\pi}} \int_Y^\infty \frac{e^{-y^2}(-2\sqrt{S})dy}{(ST)^{1/4}} = \frac{1}{\sqrt{\pi}} \int_{-\infty}^Y \left(\frac{S}{T}\right)^{1/4} e^{-y^2} dy$$

Assuming $\left(\frac{S}{T}\right)^{1/4} \approx 1$ and again breaking the integral into two parts:

$$\frac{H - H_i^*}{H_o - H_i^*} = \frac{1}{\sqrt{\pi}} \int_{-\infty}^0 e^{-y^2} dy + \frac{1}{\sqrt{\pi}} \int_0^Y e^{-y^2} dy$$

The value of the first integral is 1, so that we have finally:

$$\frac{H - H_i^*}{H_o - H_i^*} = \frac{1}{2}\left[1 + \phi(Y)\right] \equiv F \quad ----(32)$$

where $Y = \sqrt{T} - \sqrt{X} = \sqrt{bt} - \sqrt{X}$ and $\phi(Y)$ is defined as in (31), and in fact (32) is identical with (31) provided $H_i^* = 0$. This is the approximate representation of Marshall and Pigford's solution, and turns out to be the same as Jury's. Values of F may be computed with aid of tables for ϕ such as given in Lange's Handbook (14). Table I presents values of F and Figure 1 shows the same values graphically.

It is important to investigate the characteristics of the function $F = 1/2\left[1 + \phi(Y)\right]$, in order to learn how the approximate solution (32) compares with the exact solution E given by (25). The following table summarizes some of these properties and the comparison between E and F.

At X = 0;	$Y = \sqrt{T}$,	$F = 1/2\left[1 + \phi(T)\right]$	E = 1
For	T = 0,	$\phi(0) = 0$,	F = 0.5

Table I

Values of the Function $F = 1/2 \left[1 + \phi(Y)\right]$

$$\phi(Y) = \frac{2}{\sqrt{\pi}} \int_0^Y e^{-y^2} dy, \qquad \phi(-Y) = -\phi(Y)$$

Values from Lange (14).

Y	$\phi(Y)$	F
$-\infty$	-1	0
-3	-0.99998	0.00001
-2.630	-0.9998	0.0001
-2.185	-0.9980	0.0010
-2.035	-0.9960	0.0020
-1.943	-0.9940	0.0030
-1.876	-0.9920	0.0040
-1.821	-0.9900	0.0050
-1.776	-0.9880	0.0060
-1.738	-0.9860	0.0070
-1.704	-0.9840	0.0080
-1.673	-0.9820	0.0090
-1.645	-0.9800	0.0100
-1.452	-0.9600	0.0200
-1.330	-0.9400	0.0300
-1.238	-0.9200	0.0400
-1.163	-0.9000	0.0500
-1.099	-0.8800	0.0600
-1.044	-0.8600	0.0700
-0.994	-0.8400	0.0800
-0.948	-0.8200	0.0900
-0.906	-0.8000	0.1000
-0.595	-0.6000	0.2000
-0.371	-0.4000	0.3000
-0.179	-0.2000	0.4000
0	0	0.5000
0.179	0.2000	0.6000
0.371	0.4000	0.7000
0.595	0.6000	0.8000
0.906	0.800	0.9000
1	1	1

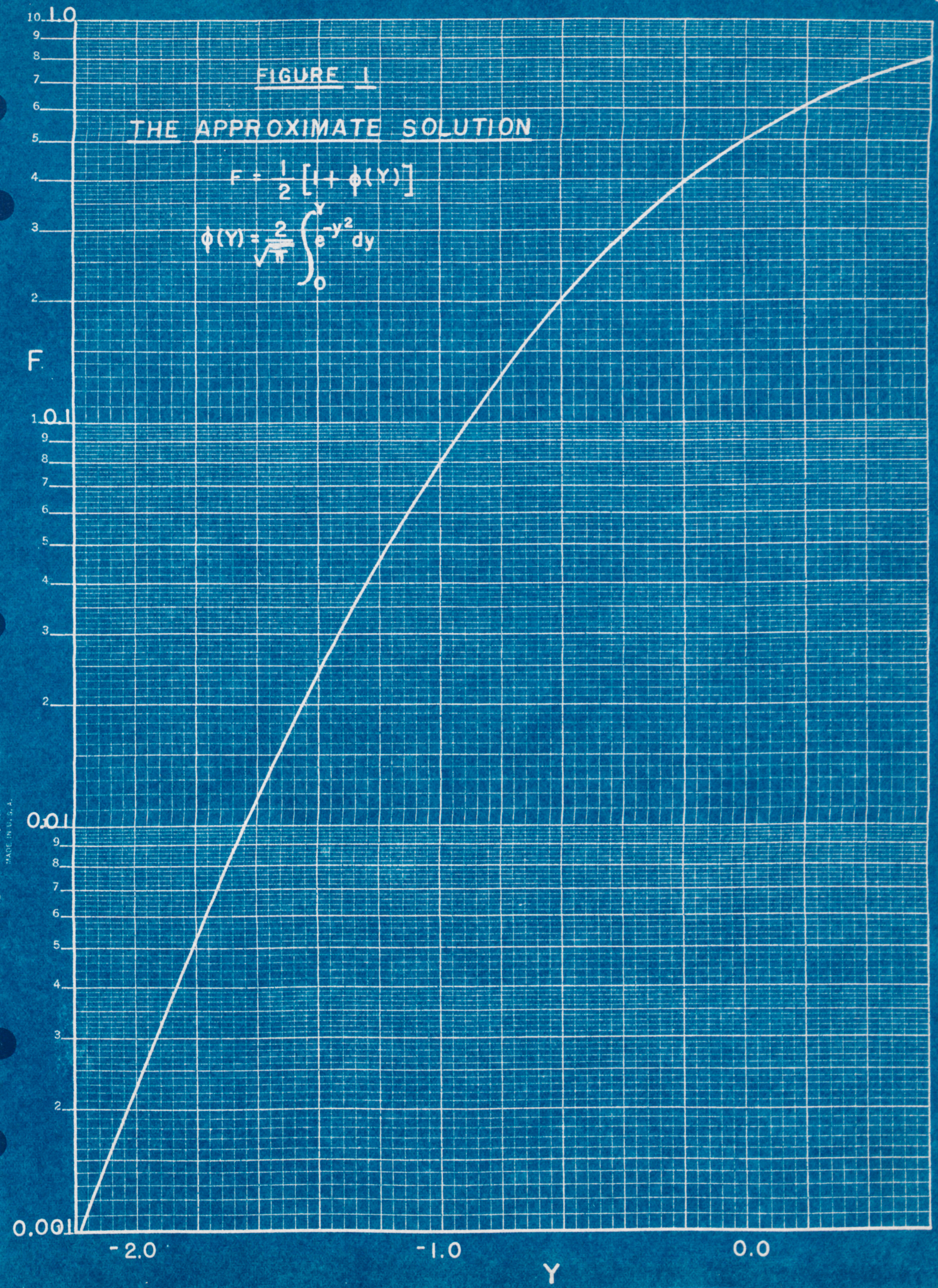
FIGURE 1
THE APPROXIMATE SOLUTION
$F = \frac{1}{2}[1 + \phi(Y)]$
$\phi(Y) = \frac{2}{\sqrt{\pi}} \int_0^Y e^{-y^2} dy$
F
1.0
0.1
0.01
0.001
-2.0
-1.0
0.0
Y

$T > 1.84$, $\phi(T) > 0.99$, $F > 0.995$

$T \to \infty$ $\phi(T) \to 1$, $F \to 1$

At $T = 0$: $Y = -\sqrt{X}$, $F = 1/2\left[1 + \phi(-\sqrt{X})\right]$; $E = e^{-X}$

For $X = 0$	$\phi(0) = 0$	$F = 0.5$	$E = 1$
$X = 1$	$\phi(-1) = -0.842$	$F = 0.079$	$E = e^{-1} = 0.368$
$X = 2$	$\phi(-2) = -0.953$	$F = 0.0235$	$E = e^{-2} = 0.135$
$X = 9$	$\phi(-3) = -0.99998$	$F = 0.00001$	$E = e^{-9} = 0.00012$

For other values of X and T, values of E and F are plotted in Figure 2. The values of E are taken from the Schuman-Furnass Chart referred to on page 25 while those of F are computed by using Table I and Figure 1. Inspection of Figure 2 shows that the agreement between E and F is fair at X = 9, but for X = 20 and above the agreement is excellent for all values of T shown.

An auxiliary curve, Figure 3, is presented to show the typical appearance of a curve which would be obtained from a bed operating with b = 0.5 and X = 100 when the data is plotted on semi-logarithmic coordinates. This is to be kept in mind when the experimental results are considered later. This curve will be typical of experimental results only, providing all the assumptions underlying the differential equation (22) are met.

Method of Testing Experimental Data:

It has been stated in the preceding section that the solution to the partial differential equation (22),

FIGURE 2

COMPARISON OF EXACT SOLUTION E WITH APPROXIMATE SOLUTION F

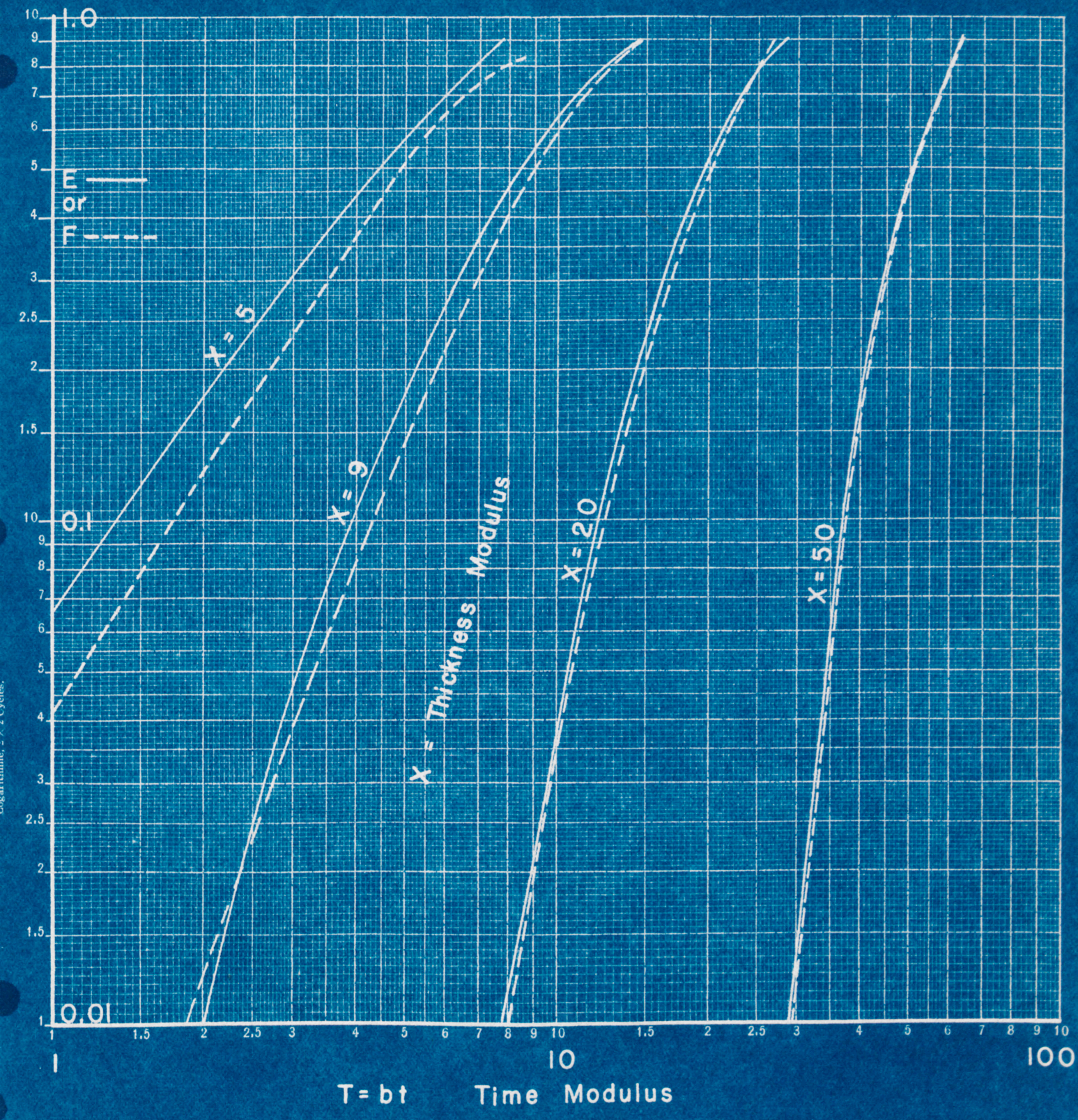

FIGURE 3

THEORETICAL PERFORMANCE OF TYPICAL BED

Conditions assumed :

$H_o = 0.001$
$W_i = 0.0002$
$B = 50$
$X = 100$
$b = 0.5$

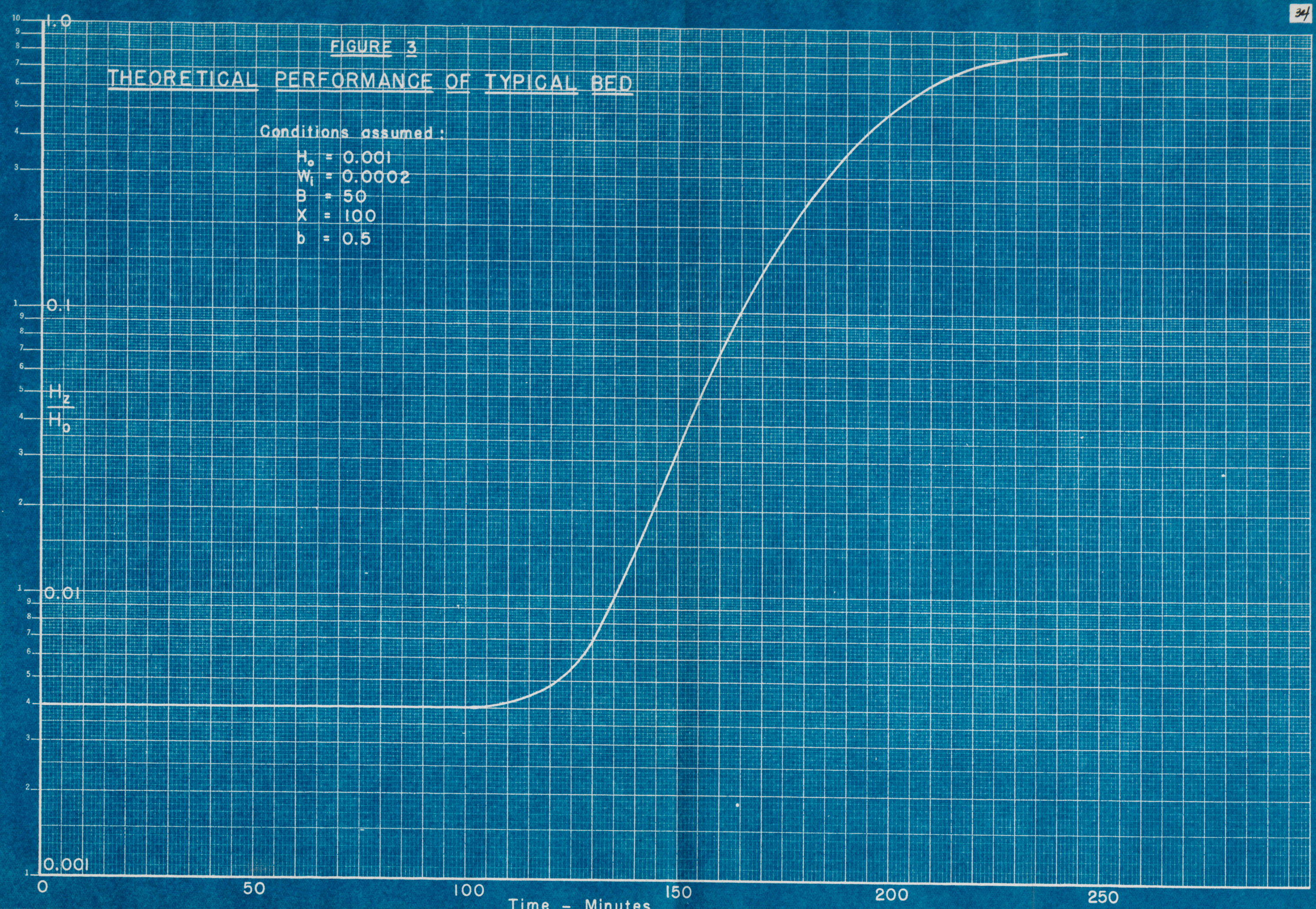

may be represented by the approximate function (32)

$$\frac{H_z - H_i^*}{H_o - H_i^*} = \frac{1}{2}\left[1 + \phi(Y)\right]$$

wherein $$\phi(Y) = \frac{2}{\sqrt{\pi}}\int_0^Y e^{-y^2}\, dy$$

and $$Y = \sqrt{T} - \sqrt{X} = \sqrt{b}\sqrt{t} - \sqrt{X} \quad ----(33)$$

Only the positive roots are to be used in Y. According to the assumptions underlying this equation, b and X are both constant for a given run.

It is desirable to have a simple method of testing experimental data of H_z vs. t in order to determine whether this equation applies to the bed performance, and if so to determine numerical values of b and X for a particular run. This may be accomplished in the following way.

It is evident that $\frac{H_z - H_i^*}{H_o - H_i^*}$ is a single-valued function of Y which, in turn, is a single-valued function of t. If this equation applies, the relationship between $\frac{H_z - H_i^*}{H_o - H_i^*}$ and Y is always the same regardless of the conditions in a particular run. This relationship has been presented in Table I and Figure 1. It is to be noted that Y may have both positive and negative values and that $\phi(Y)$ is an odd function, i.e., $\phi(-Y) = -\phi(Y)$.

Now Y is linear in $\sqrt{t}$. A plot of Y vs. $\sqrt{t}$ should be a straight line having a slope equal to $\sqrt{b}$ and an ordinate

intercept equal to $-\sqrt{X}$, if the theory applies. Accordingly, the following steps should be followed to test a set of data of H_Z vs. t.

1) Calculate values of $\frac{H_Z - H_i^*}{H_o - H_i^*}$. This requires a value for H_i^* which may be estimated from the initial moisture content of the bed W_i if the adsorption constant B is known. In many cases, if the bed has been properly prepared, W_i and H_i^* may be very small but the values of H_Z will be of the same order of magnitude at the beginning of the run. The very first measured value of H_Z may be very close to H_i^* if the sampling and testing has been quickly and carefully done.

2) Plot the data with $\frac{H_Z - H_i^*}{H_o - H_i^*}$ as ordinate and t as abscissa. It has been found most convenient to use a semi-logarithmic plot, wherein $\log \frac{H_Z - H_i^*}{H_o - H_i^*}$ is plotted against t in order to cover the range of values of $\frac{H_Z - H_i^*}{H_o - H_i^*}$ which usually lies between 0.001 and 1.

3) Draw the best smooth curve through these plotted points.

4) Select a series of values of $\frac{H_Z - H_i^*}{H_o - H_i^*}$ and read from the smooth curve the corresponding values of t. It is most convenient to select a series of rounded values such that $\frac{H_Z - H_i^*}{H_o - H_i^*}$ is 0.006, and 0.008, 0.01, 0.02, 0.04, 0.06,

etc., as needed to cover the range.

5) From Table I obtain the values of Y corresponding to the values of $\frac{H_z - H_i^*}{H_o - H_i^*}$ selected. Values of Y may also be read from Figure I but less accurately.

6) Plot the values of Y (as ordinate) selected in step 5 against $\sqrt{t}$ (as abscissa) computed from the values of t obtained in step 4.

7) Draw the best smooth line through the points plotted in step 6. If this is a straight line, conformity of the data to the equation (33) is established. From the plot determine the slope and the ordinate intercept of the straight line, and calculate:

$$\left.\begin{aligned} b &= (\text{slope})^2 \\ X &= (\text{ordinate intercept})^2 \end{aligned}\right\} \quad - -(34)$$

If it is not convenient to determine the intercept itself, X may be calculated by selecting any point on the line, say (t_1, Y_1) and computing

$$X = (\text{slope} \cdot t_1 - Y_1)^2$$

We then have a rather simple and direct graphical method of testing the applicability of equation (32) to describe test data. This method has been used to test data obtained by Jury (11) as well as all new runs obtained by the author.

If a fairly good straight line should be obtained by this test, but it should have a value of X^- less than about 20, then the test is not conclusive because the approxi-

mate function does not represent the rigorous solution so well for $X < 20$.

It would be necessary to test the data further against the Schuman-Furnass Chart itself. However, in such a case, the value of X obtained from the straight line may at least serve as a starting point for the trial and error procedure of testing against the chart.

From the values of b and X obtained by the testing procedure, the value of the resistance r may be found, and also a value for 13. For, referring to page 23, equations (21) and (22)

$$X = \frac{\rho_B Z}{GX} \qquad \text{and} \qquad b = \frac{1}{r_B}$$

so that

$$r = \frac{\rho_B Z}{GX}$$

and

$$B = \frac{GX}{\rho_B Z b}$$

The value of B obtained here should be checked against that obtained by static equilibrium experiments. Since it is more convenient to work with values of b and X, especially if the Schumann-Furnas Charts must be used, we shall discuss the interpretation of the data in terms of b and X rather than r and B.

Interpretation of Experimental Data

If experimental data from one run are tested according to the method just described, and yield a straight

line plot for Y vs. $\sqrt{t}$, it means that they fit functions (32), the approximation to the solution of differential equation (22). If the value of X found from the test is large enough so that the approximate solution is a sufficiently accurate representation of the rigorous solution (25), then the data must follow this differential equation. Since several different kinetic relationships may each give this same form of differential equation, however, it is impossible to determine from one run which type of resistance is involved. It will be necessary to make a number of runs in which some important variable, such as flow rate, particle size, bed and air temperature, air pressure, etc., is changed and to observe the effect of these changes upon the values of b and X obtained from each run.

From the kinetic relationships presented, we have the following expression for b and X in each case.

	X	b
Mass transfer	$\frac{K_G a_v}{G} Z$	$\frac{K_G a_v}{\rho_B B}$
Internal diffusion	$\frac{\pi^2 B D_I \rho_B}{R^2 G} Z$	$\frac{\pi^2 D_I}{R^2}$
Shell diffusion	$\frac{K_s a_v \rho_B B}{G} Z$	$K_s a_v$

From these in turn, using also the facts known about K_G, D_I, and K_s, we may deduce the effect of important operating variables upon b and X. This is presented in the table on the next page.

Table II
Effect of Operating Variables upon Constants b and X

Variable		Case 1. Mass transfer	Case 2. Internal diffusion	Case 3. Shell diffusion
Mass velocity G	$X \propto$	$\frac{d}{G^n}$	$\frac{1}{G}$	$\frac{1}{G}$
	$b \propto$	dG^{1-n}	constant	constant
Particle size: R	$X \propto$	$\frac{d}{R^{1+n}}$	$\frac{\rho_B}{R^2}$	$\frac{K_s \rho_B}{R}$
	$b \propto$	$\frac{d}{\rho_B R^{1+n}}$	$\frac{1}{R^2}$	$\frac{K_s}{R}$
Bed length Z	$X \propto$	Z	Z	Z
	$b \propto$	constant	constant	constant
Temperature (Assumed to be the same for the bed and the air stream)	$X \propto$	$\frac{d(\rho_f D_{A_m})^{2/3}}{\mu^{2/3-n}}$	BD_I	BK_s
	$b \propto$	$\frac{d(\rho_f D_{A_m})^{2/3}}{B\mu^{2/3-n}}$	D_I	K_s
Pressure of Gas	$X \propto$	$\frac{d(\rho_f D_{A_m})^{2/3}}{\mu^{2/3-n}}$	B	B
	$b \propto$	$\frac{d(\rho_f D_{A_m})^{2/3}}{B\mu^{2/3-n}}$	constant	constant
Humidity H_o	$X \propto$	$\frac{d(\rho_f D_{A_m})^{2/3}}{\mu^{2/3-n}}$	constant	constant
	$b \propto$	$\frac{d(\rho_f D_{A_m})^{2/3}}{\mu^{2/3-n}}$	constant	constant

For example, if a series of runs is made in which only mass velocity is varied, and if for each run a straight line plot of Y vs. $\sqrt{t}$ is obtained, and if, further, the values of X are found to be inversely proportional to $\frac{1}{G}$, while those of b are all the same, we may conclude that either internal diffusion alone or shell diffusion alone is a sufficient explanation for the bed behavior. However, if the values of X are proportional to $\frac{d}{G^n}$ and those of b are proportional to dG^{1-n} using values for d and n as given on page 12, then mass transfer alone is a sufficient explanation for the bed behavior.* If the first possibility occured, then a further test to distinguish between internal diffusion and shell diffusion could be made by running a series of tests with different particle sizes. For internal diffusion, X and b are both inversely proportional to R^2, while for shell diffusion they are inversely proportional to R, provided that correction is made in bulk density of the bed.

If one of the above described possibilities is identified, we may be satisfied with the corresponding sufficient (though not necessary) explanation for the bed behavior, at least for design purposes. However, two other

---

*This is only true provided the flow is turbulent. For viscous flow $n = -2$ and $X \propto \frac{1}{G}$ for mass transfer also.

possibilities must be considered: The test lines of Y vs. $\sqrt{t}$ may not be straight; the lines may be straight but the values of X and b may not fit into any of the patterns indicated in the table.

If the lines of Y vs. $\sqrt{t}$ are straight, but the variations in X and b do not accord with any of those in the table, it means that the kinetic relationship follows equation (18), in which r and B are constant, but that none of the three individual types of resistances discussed is <u>alone</u> responsible for the bed behavior. We would then have a combination of resistances, the overall effect of which remains constant throughout the run.

If the lines are curved, it means that at least one resistance varies during the run. A common case might be a plot which is straight over the lower portion and curves upward at the top. This might be explained by very rapid internal diffusion at the beginning so that the mass transfer equation was followed at first, but with internal diffusion becoming very much slower at the end so that the total resistance was appreciably increased and the rate of exhaustion of the bed capacity became increasingly greater. Or it might be simply a case of internaldiffusion controlling throughout, but with the coefficient D_I decreasing as the bed becomes saturated.

The experimental work undertaken in this investigation has been of such a nature as to attempt to determine along these lines which resistances are involved in the calcium sulphate system.

Experimental Work

Review of Tests Made by Jury

Jury (loc. cit.) made some twenty test runs in which values of H_z were measured with the frost-point hygrometer against time. All of these runs were made on beds 1" diameter packed with commercial Drierite. The length of the beds varied from 2" to 9", the rate of flow of air from 417 cu. ft. per hour to 9.4 cu. ft. per hour, and the particle size from 2-2 1/2 mesh to 20-24 mesh. (Tyler standard screen sizes). In all runs the value of H_o was virtually the same at 1320 x 10^{-6}, ratio of mass of water to mass of air (absolute humidity). Details of the apparatus used are given in Jury's thesis.

Jury plotted the data from these tests in the form of log H_z/H_o vs. t. with no account being taken of H_i^*. An inspection of these graphs reveals several interesting facts. Very few of them actually follow the general form of Figures 2 or 3. The initial portion of the runs almost always shows a gradually decreasing H_z/H_o. Most of them exhibit points of inflection and some of them have one or more flat regions in which H_z/H_o remains rather constant for a time and then abruptly rises. The accompanying sketches show typical samples.

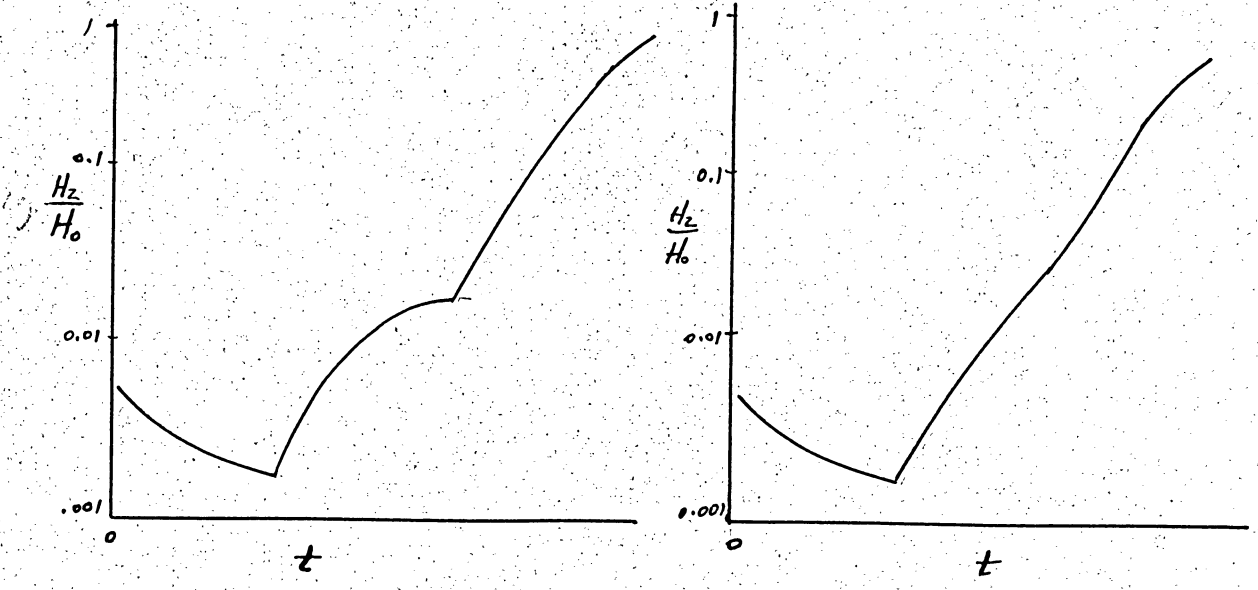

The initial decrease is readily accounted for by the fact that the pipe lines leading from the outlet end of the bed to the hygrometer are being purged and dried out by the very dry air issuing from the bed at the beginning. This effect was accentuated by the presence of a steel wool filter pad just behind the granules at the outlet end. This filter evidently was capable of holding considerable adsorbed moisture for when it was removed the initial decrease period was appreciably shortened. It was subsequently decided that such a filter was really not needed and all later runs were made without it.

Obviously such curves will not be in accord with the equations for H_z/H_o (assuming $H_i^* = 0$) developed in the preceding section. Jury attempted to determine the nature of the rate-controlling resistance, however, by testing his data against the Schuman-Furnas charts (9) to test them. While recognizing the discrepancies which existed he nevertheless drew the tentative conclusion that internal diffusion of water within the desiccant granule was the rate-controlling step.

The author applied his method of testing (assuming $H_i^* = 0$) as described on pages 32-38 and, of course, found very poor agreement with the theoretical equation. The plots of Y vs $\sqrt{t}$ cannot possibly be straight lines when there is a flat region or point of inflection in the graph. The question naturally arose as to whether it was the theory or the experimental work which was incorrect. It was evident that further

study of the problem was required, and it became the principal purpose of this investigation to attempt to answer the question. We shall discuss next the experimental approach and finally the interpretation of experimental results in the light of the theory already presented.

General Experimental Procedure; Preliminary Runs.

In order to seek possible errors in the experimental work it was necessary to review the general procedure heretofore employed. Some fifteen runs were made by the author using Jury's methods in an attempt to become familiar with the technique and to duplicate his results. Briefly the procedure followed in each run was as follows:

1) Regenerate the desiccant to be used. During screening and handling even fresh, unused material has an opportunity to pick up moisture from the air. It is necessary to have the desiccant as dry as possible in order to obtain fulluse of its available capacity for absorbing water vapor in the test bed. According to the recommendations of the manufacturers of Drierite, this may be accomplished by heating the desiccant for several hours at 400 - 425°F.* Originally, this was done merely by spreading the material (of a certain grain size) out in a shallow pan and placing it in a muffle furnace controlled to 420 ± 5°F

*If the material is overheated it becomes permanently inactive.

by a thermocouple suspended over the pan. Fresh material was reactivated and used for each run and discarded thereafter.

2) Load the bed container. This was done simply by pouring the hot desiccant, directly after it was removed from the furnace, into the short pipe nipple which served as a bed container. The pipe was tapped and shaken to pack the granules well and then immediately capped and sealed at the joints with beeswax. It was allowed to cool to room temperature before using.

3) Insert the loaded container into the test apparatus. The inlet end was connected to a source of compressed air of controlled humidity through a calibrated rotameter to measure the rate of air flow into the bed. The outlet end was connected directly to the frost-point hygrometer. Provision was made to by-pass the feed air around the bed to the hygrometer in order that H_o could be measured.

4) Adjust the air supply to the desired humidity H_o. This was done by passing the compressed air, at regulated pressure, through a long coil immersed in an insulated ice chest where the temperature was held at 32°F. Since the air supply always contained more water vapor than saturated air could hold at 32°F and the pressure maintained, moisture condensed in this

coil and was removed periodically through a trap. The air supply issuing fromthe ice-coil was thus at a constant humidity which could be varied within limits and controlled merely by setting the pressure at a specified value.

5) Prepare the frost-point hygrometer for use. This involves merely filling the cold bath container with a mixture of solid carbon dioxide and methyl alcohol, and turning on the electrical circuits. The principle of this hygrometer is simply that of determining whether a deposit of moisture will form when the air is passed over a gold plated surface which is held at a certain temperature. The temperature of the surface is controlled by a combination of the cooling bath and an electric heating element. The deposition of moisture is detected by changes in the diffuse reflection of a constant light source shining on the surface, as observed by a photoelectric cell. For complete details on the construction of this instrument, the reader is referred to Jury's thesis. The technique of making the measurements with it will be discussed in detail on page 59.

6) Measure the humidity of the feed air supply and then turn it into the bed. Atthis instant begin to count time.

7) Measure the humidity H_z of the air issuing from the

bed at intervals of time until the bed is nearly exhausted, i.e. until H_z has risen to become nearly equal to H_o.

The results obtained in the preliminary runs made according to this procedure were quite erratic and unsatisfactory. For this reason none of this data is reproduced here. Long, flat portions and points of inflection were commonly obtained on the graphs, although the initial gradual decrease of H_z was practically eliminated by the removal of the steel-wool filters as mentioned above. In addition, erratic values of H_o were obtained in spite of the fact that no known changes were made in the settings of the apparatus which was supposed to control H_o.

Careful consideration was given to each of the steps in the procedure as listed above for possible sources of error. In regard to steps (1), (2), and (3) it was felt that the method of regeneration, or reactivation, and loading of the bed container might be a source of difficulty. The heating and circulation of air over the bed in the furnace might be erratic and the particles in the layers underneath the surface might not be properly exposed. Further, the contact with the air of the room during loading might have a deactivating effect. We could not be certain that every bed prepared would be in identically the same condition at the beginning of the test run. Successful regulation of H_o, as

in step (4), depends upon a close control of the pressure of the air passing through the coil immersed in the ice chest, and upon cooling of the air completely to 32°F all the time. Droplets of vapor condensed in this coil might remain suspended in the air stream and give an abnormally high humidity. Further, the air supplied to the ice-chest dehumidifier must always have a greater humidity than corresponding to saturation under the controlled conditions, otherwise an abnormally low value would be obtained as no condensation would occur in the coil. Finally, the operation of the hygrometer, steps (5), (6), and (7), must be carefully studied. It was not evident at the outset what errors might be introduced here.

New Method of Regeneration of Bed

To eliminate the objections mentioned in connection with steps (1), (2), and (3), a new method of regeneration was installed. This consisted of packing the bed container first and installing it in the test line. The test line was so arranged that the bed could be immersed in an oil bath which could be heated and controlled at any desired temperature up to about 450°F (limited only by the flash-point of the oil). A current of dry air, preheated to the bath temperature by passage through a coil also immersed in the same bath, was swept through the bed during the heating period. This provided for carrying off the moisture liberated from the

granules. At the end of the heating period the oil could be drained from the bath and the bed allowed to cool slowly. All lines to the bed would then be closed except a "breather" line which permitted room air to enter through a large auxiliary bed of desiccant. This was necessary to prevent moist room air from leaking in during cooling, and governed to some extent the value of H_i^*. After the bed was cool, the inlet and outlet lines could be opened, the breather line closed, and a regular run made without disturbing the granules at all. Thus all the objections to the furnace method were eliminated. Figure 4 shows schematically the apparatus used. The details on construction of the bed container assembly are shown in Figure 5. It is believed that these drawings are sufficiently complete and self-explanatory that further description of this equipment is unnecessary.

The progress of the regeneration could be followed by measuring the humidity of the air stream leaving the bed. If the granules contained much moisture, this would rise quite rapidly as the bath heated up. After a time a peak would be reached and then the humidity would decrease to the same value as that of the inlet air stream.

After a few preliminary trials the following method was adopted as a standard regeneration. With the entire apparatus at room temperature the air stream and the immersion heaters were turned on together and the controller was set for 410°F. The air stream was adjusted to flow at the rate

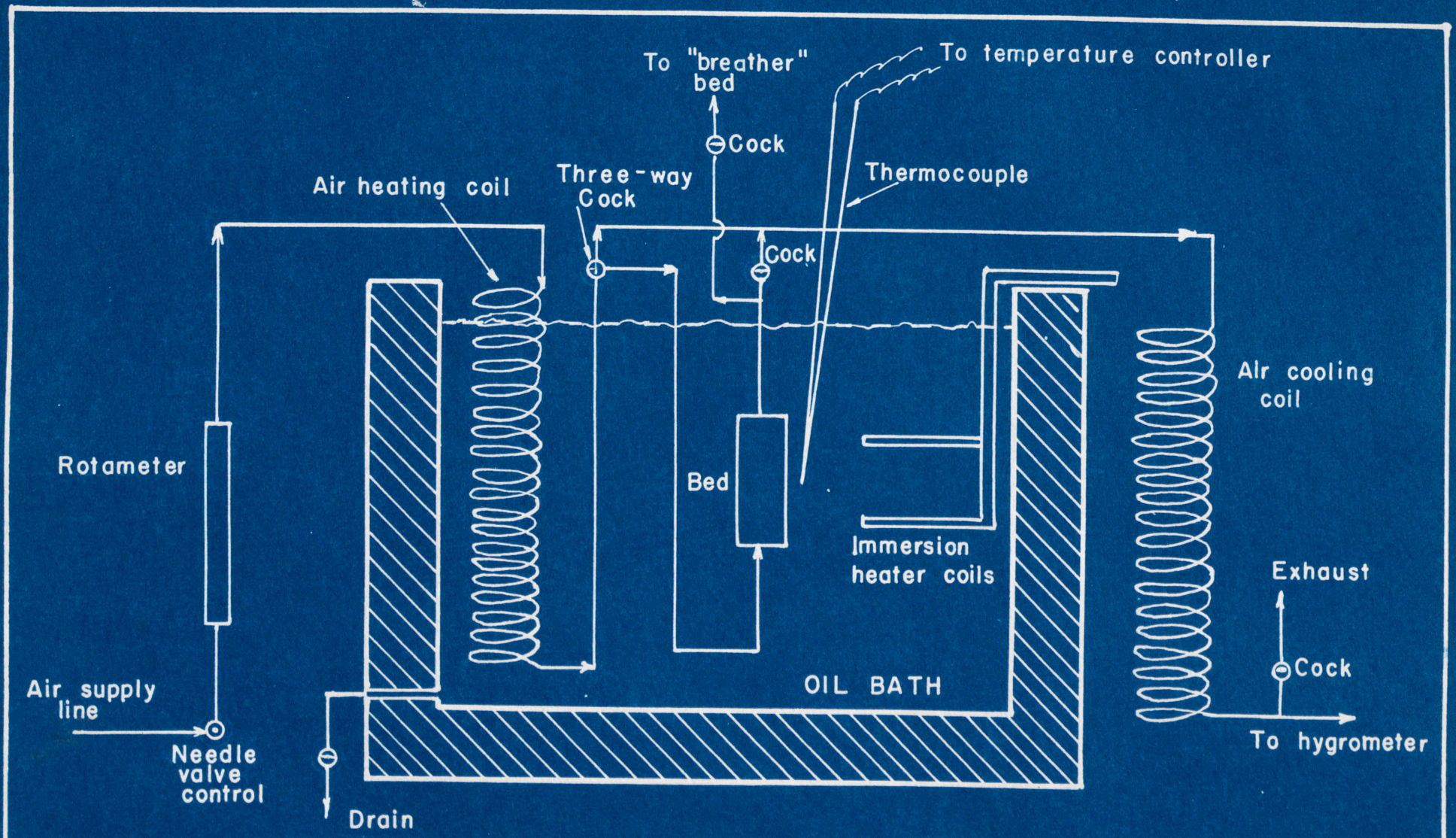

FIGURE 4

REGENERATION APPARATUS

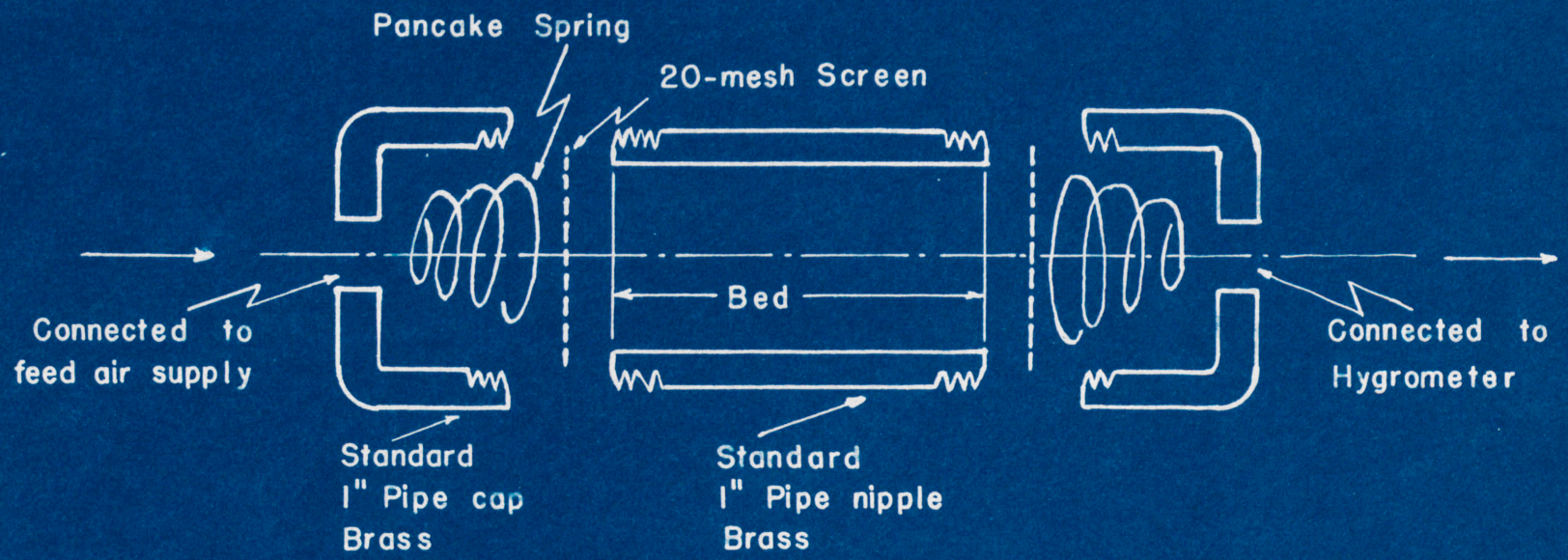

FIGURE 5

BED CONTAINER ASSEMBLY

of 9.4 cu. ft. per hour. It required approximately 1-1/2 hours for the bath to reach temperature after which the controller held it at 410 ± 5°F. as measured by the thermocouple which actuated the controller, as well as by a mercury thermometer immersed next to the bed container. After the hygrometer showed that the outlet humidity had fallen to that of the inlet air, and the bath was at 410°F, heating was continued for one hour longer. The total length of time required from the start wasusually three hours. At this time, the heaters and the air stream were turned off, the breather line opened, and the hot oil drained from the bath. The subsequent natural cooling required at least four hours, but the bed was always allowed to stand over night before use in a test run. If it was desired, the same bed could be regenerated and tested again and again without disturbing it.

No extensive investigation into the regeneration process was attempted. The method outlined above was simply arbitrarily adopted and used for all runs made by the author. It is felt, however, that further study of the effect on regeneration of variables such as temperature of bath, temperature of air, rate of flow of air, humidity of inlet air, cycle of heating and cooling, etc. would be desirable.

Control of Humidity of Air Feed Supply

As explained above in connection with step (3) of the experimental procedure, the humidity of the air feed stream was controlled by bringing it to saturation at a

definite temperature and pressure. Since it was always cooled in an ice chest, it was assumed that the temperature was about 32°F. The pressure could be varied by adjusting a reducing valve in the line just ahead of the ice chest. The pressure was read on a Bourdon gauge just below this valve, the gauge being capable of reading from 0 to 60 lb. per square inch above atmospheric pressure (psig) in scale divisions of 1/4 lb. per sq. in. It was recalibrated against a dead-weight gage tester before installation.

The source of air was the storage tank of a compressor in which the pressure varied from 100 to 150 psig during the on-off cycle of the compressor operation. This tank stood in a room where the temperature averaged 70°F and certainly never fell below 60°F. Hence the driest condition of the air in this tank, corresponding to saturation at 60°F and 150 psig, was an absolute humidity of 9.64×10^{-4} pounds water per pound of dry air. This value is calculated from the vapor pressure of water at 60°F of 0.256 psia as given by Keenan and Keyes (12), according to the formula:

$$H = \frac{18}{29} \frac{p}{P-p} = \frac{18}{29} \times \frac{0.256}{(165-0.256)} = 9.64 \times 10^{-4} \quad --(35)$$

H = absolute humidity

p = vapor pressure of water at saturation temperature, psia.

P = total pressure of the air, psia.

To help smooth out the fluctuating pressure from the compressor a second reducing valve was installed in the line

ahead of the first valve. This reduced the pressure from 100 - 150 psig to approximately 60 - 80 psig. The first reducing valve reduced it further to the desired pressure, in most runs at 40 psig, and there was only a barely visible fluctuation of the pressure, much less than 1/4 psi in either direction. The assembly is shown in the accompanying Figure 6.

Table III below shows the value of the absolute humidity of air saturated at various gage pressures, and at 32°F. Depending upon the setting of the reducing valves, this should be the humidity of the air fed to the bed under test, provided complete cooling of the air to 32°F was obtained without supersaturation and provided there were no suspended droplets. (A glass wool filter was installed in the trap in the ice-chest in order to eliminate this latter possibility.) Table III also gives values for saturation at 33°F, for consideration in the event that cooling of the air was not complete. All of these values given here were calculated from equation (35) for H stated above, assuming an average barometric pressure of 14.4 psia and using the vapor pressure of water given by Keenan and Keyes (12). It is evident that all of these values are much smaller than that stated in the preceding paragraph for the driest condition possible in the compressor tank. Consequently, condensation will always occur in the coil immersed in the ice chest, and this arrangement should insure a supply of air at constant

FIGURE 6

AIR SUPPLY HUMIDITY CONTROL

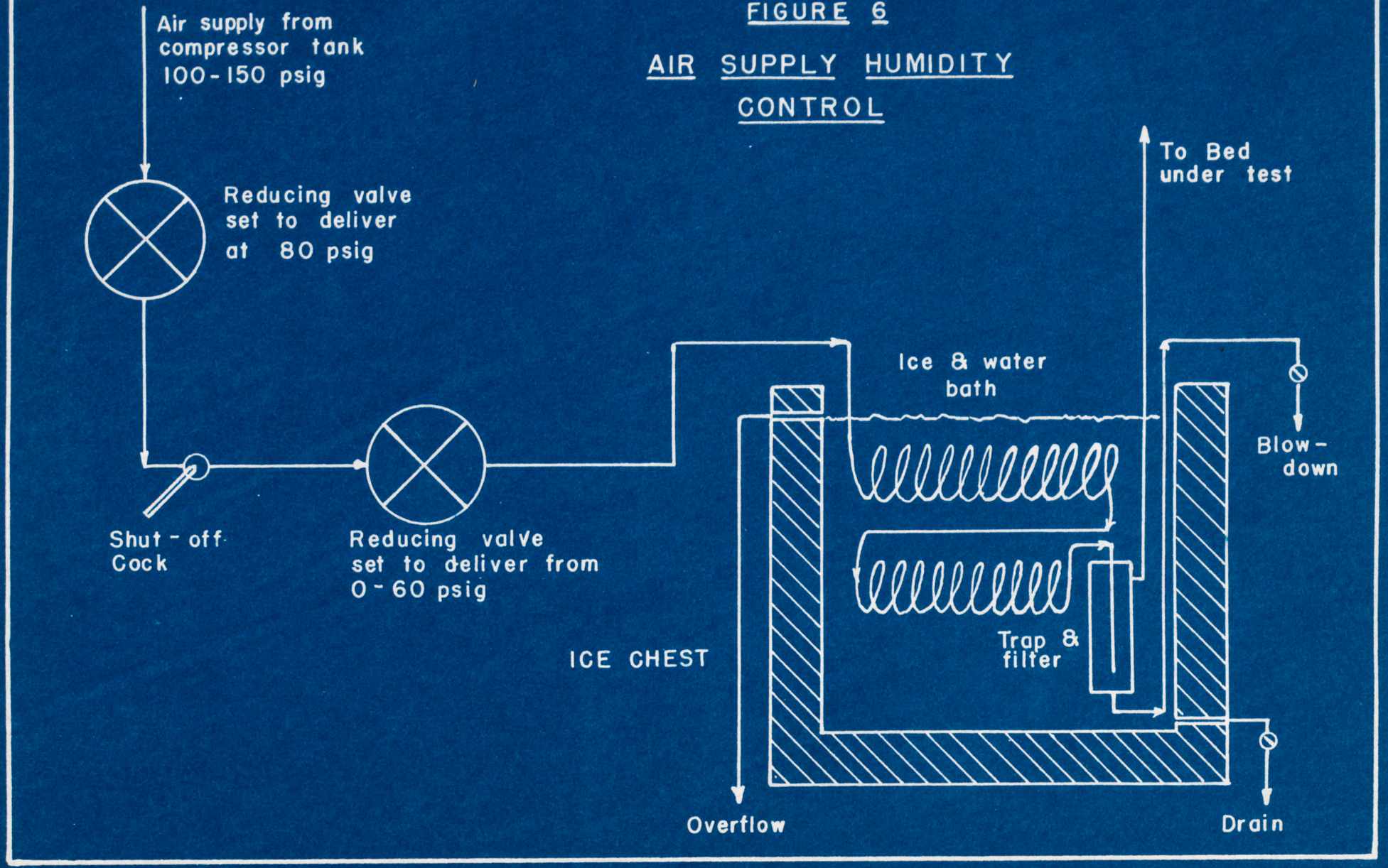

Table III

Absolute Humidity of Feed Air Supply

Gage Pressure-psi	Absolute° Pressure-P psi	Temp.* -°F	Absolute Humidity-Hx10^6
0	14.4	32	3840
		33	4010
10	24.4	32	2260
		33	2360
20	34.4	32	1550
		33	1670
30	44.4	32	1237
		33	1289
40	54.4	32	1012
		33	1054
50	64.4	32	855
		33	891
60	74.4	32	739
		33	771

*Vapor pressure of water at 32°F: p = 0.08854 psia
Vapor pressure of water at 33°F: p = 0.09223 psia

°Based upon a barometric pressure of 14.4 psia.

humidity.

During the preliminary runs, determinations of the humidity of the air supply made with the Jury frost-point hygrometer did not agree with the values stated in the table. The factors affecting pressure and temperature control as described above were carefully reviewed and some adjustments made but to no avail. It was subsequently discovered that the fault was in the technique of using the hygrometer. When this was corrected, the determination agreed well with the calculated values at 32°F, and it was established that the control of the humidity of the air supply was closer than the ability of the instrument to measure it. Values of H_o were then taken from Table III for use in subsequent calculations. The correct technique of using the hygrometer is discussed thoroughly in the next section.

Technique of Using the Frost Point Hygrometer

To operate the frost-point hygrometer it is necessary to cool the gold-plated surface until a deposit forms from the sample of air flowing over it. When the current in the heating element just below the surface is reduced (by an electronic rheostat), cooling occurs because the surface is on one end of a copper rod which is immersed in a bath consisting of lumps of solid carbon dioxide, in methyl alcohol. Hence the surface temperature is regulated by control of the heater current. Since super-cooling of the air stream may

occur, it is necessary to warm the surface after the deposit forms until a temperature is reached at which the deposit neither increases nor decreases. Any change in the size of the deposit is indicated by a change of current in the photoelectric cell which views the light diffusely reflected by the deposit, the current therefore being greater the larger the deposit. The desired point of equilibrium between deposit and air is thus indicated by a constant photocell current. It may be approached either by cooling the surface very gradually until a light deposit just forms and then warming very slightly, or by rapidly cooling to a temperature far below that necessary, obtaining a heavy deposit and warming fairly rapidly, i.e., approaching either from the high side or low side. The temperature of the surface at equilibrium is measured by a thermocouple imbedded in it and connected to Leeds and Northrup Precision Potentiometer capable of reading to 0.01 millivolt, which corresponds to 0.5°F. The calibration data for this thermocouple is given in the Appendix.

The significance of the equilibrium surface temperature depends upon the nature of the deposit. Either ice or water may form, as frost or dew respectively. The appropriate vapor pressure of the deposit must be used to compute the humidity of the air stream in equilibrium with it. Since the surface is at atmospheric pressure, the following formula applies:

$$H = \frac{18}{29} \times \frac{p}{P-p} \qquad \ldots\ldots\ldots\ldots (36)$$

wherein H = absolute humidity of air stream

p = vapor pressure of deposit at temperature of surface, psia

P = atmospheric pressure, barometer reading, psia.

The range of temperature over which the surface may be controlled with a solid carbon dioxide bath runs from about -90 °F with the heater completely off to about + 32°F with full heater current. Hence, data on the vapor pressure of water and ice are needed over this range. Tables V and VI in the appendix present values of H calculated from vapor pressure of ice and water respectively. These dataare discussed below in the next section on page 75 .

In the preliminary runs and tests of the humidity of the feed air supply, the fact that supercooled water might deposit at temperatures below 32°F was not fully appreciated. Consequently, erratic readings of the "frost-point" or "dew-point" corresponding to H_o were obtained and were assumed always to correspond to ice deposits. The erratic readings were erroneously attributed to variations in the condition of the air supply. Later it was learned by experience that the nature of the deposit was likely to be water at any temperature above -40°F when equilibrium was approached from the low side provided the initial rapid cooling was to -40°F or below. However, this was not an entirely consistent performance and it was found that the only certain way to ascertain the nature of the deposit was to examine it visually.

Fortunately, the optical head of the hygrometer was built with an extra hollow tube which could be opened and through which the lighted gold surface could be viewed, preferably with the aid of a hand lens. After some practice, it became possible to distinguish the nature of the deposit and in all later tests this observation was made and recorded. When this was done, the apparently erratic nature of the determinations of H_o disappeared. The following data are cited as typical examples.

Determinations of Humidity of Feed Air Supply

November 7, 1949

Air supply pressure = 29 psig, uncorrected gage reading.
Rate of flow of air = 9.4 cu. ft. per hour, through hygrometer.

Time - PM	Thermocouple mv	Reading °F	Probable Nature of Deposit*
1:12	0.57	+4.5	water
1:17	0.51	+7.5	ice
1:44	0.57	+4.5	water
1:46	0.57	+4.5	water
2:03	0.59	+3.5	water
2:45	0.51	+7.5	ice
3:00	0.56	+5.0	water
3:30	0.52	+7.0	ice
3:39	0.55	+5.5	water
3:40	0.56	+5.0	water
3:58	0.50	+8.0	ice
4:10	0.50	+8.0	ice
4:28	0.51	+7.5	ice

The absolute humidity corresponding to average water deposit = 1167 x 10^{-6} at +4.5°F, and 14.4 psia, the absolute humidity corresponding to average ice deposit = 1175 x 10^{-6} at +7.5°F

*This was not actually observed at the time, but is deduced from the temperature readings.

and 14.4 psia. The calculated humidity of air supply at 43.4 psia (29 psig) and 32°F = 1265 x 10^{-6}. (This disagreement was later discovered to be due to the fact that the calibration of the pressure gage was in error.)

December 8, 1949

Air supply pressure = 30 psig, corrected gage reading (recalibrated).
Rate of flow of air = 9.4 cu. ft. per hour, through hygrometer.

Time - PM	Thermocouple Reading mv	°F	Probable Nature of Deposit	Humidity x 10^{-6} (14.4 psia)
2:12	0.55	+5.5	water	1222
2:24	0.55	+5.5	water	1222
3:25	0.55	+5.5	water	1222
3:35	0.56	+5.0	water	1188

Calculated humidity of air supply at 14.4 psia and 32°F = 1237 x 10^{-6}.

January 16, 1950

Air supply pressure = 40 psig, corrected gage readings (recalibrated). Rate of flow of air = 9.4 cu. ft. per hour, through hygrometer.

Time - PM	Thermocouple Reading mv	°F	Probable Nature of Deposit	Humidity x 10^{-6} (at 14.4 psia)
12:25	0.65	+1.0	water	996
12:42	0.65	+1.0	water	996
12:57	0.65	+1.0	water	996
1:36	0.55	+5.5	ice	1065
1:43	0.55	+5.5	ice	1065
1:45	0.55	+5.5	ice	1065

Calculated humidity of air supply at 54.4 psia and 32°F = 1012 x 10^{-6}.

These figures show that the instrument is capable of measuring the dew point or frost point within 0.5°F, and that if the nature of the deposit be properly identified, the humidity may be determined to about within 3% of the

calculated value on the average.

It was quite surprising to the author to learn that liquid water might be deposited as dew at temperatures as low as -40°F, and not crystallize immediately into ice. This observation was corroborated by Brewer, Cwilong, and Dobson (2), and Suomi (18). The former state:

> "If the surface is polished and clean, dew will generally be deposited down to temperatures as low as -40°C, while by taking special precautions, it is possible to form dew on a solid surface at any temperature down to -100°C. If the surface is not very clean, ice may be formed at temperatures well above -40°C."

The latter states:

> "The lowest temperature at which supercooled liquid was observed is -35°C. Except in the 0 to -30°C range the instrument normally operated with ice on the mirror. Schaeffer (16) suggests that if the mirror is covered with a microscopically thin layer of polystyrene, the instrument will always operate with supercooled water at temperatures above -35°C., and with ice below that temperature, thus eliminating ambiguity."

Recently, a study has been made by Heverly (7) on the spontaneous freezing points of supercooled droplets of water. He found that the freezing point was dependent upon the size of the droplets, but was independent of the source of the water, the rate of cooling, or of the pressure. For drop diameters of 1.1 - 0.4 mm., the spontaneous freezing point was practically constant at -16°C. Below 0.4 mm., the spontaneous freezing point decreased to -30°C. for a diameter of 0.06 mm., and the rate of

decrease of freezing point with decreasing drop diameter varied inversely with the drop size. In the operation of the Jury hygrometer, it is certain that very small droplets will form upon condensation from the vapor state. Hence, the fact that we found water to exist ordinarily at temperatures down in the neighborhood of -40°F. (which is the same as -40°C.) is in general accord with Heverly's observations.

Realization of the facts just stated brought about a further very important modification in the technique of making determinations during the test runs of a bed. Originally, in all the preliminary runs, and presumably, also in the runs made by Jury, the technique was as follows. At the beginning of a run the humidity of the outlet stream would, of course, be very low. The heater current would be turned way down, in some cases completely off, and the initial deposit would form in the neighborhood of -80°F in most cases. This deposit was undoubtedly ice although it was not observed directly at the time. This reading and the humidity would remain rather constant for a while but sooner or later the bed would "break", that is the humidity H_z would begin to rise. From then on the temperature of the surface had to be continually adjusted to keep pace with the rising humidity. Originally, this was done by raising the temperatures somewhat until the deposit began to decrease, but not enough to evaporate it completely. The

The current in the photoelectric cell circuit would decrease gradually and finally come to a steady value for a few moments as the increasing humidity "caught up with" the higher temperature. Then this current would begin to increase again as the deposit grew heavier. Finally, the temperature would be stepped up again beyond the value corresponding to the humidity at the moment and evaporation would begin again. This cycle of increasing temperature, watching photocell current decrease, become stationary and begin to rise, followed by another temperature increase, was repeated over and over as the bed gradually became exhausted. At no time was the surface cleaned completely of all deposit. The point of stationary photocell current was taken as an indication of equilibrium between the deposit and the air, and the time and temperature noted as a reading. The deposit was assumed to be ice at all times and the humidities calculated accordingly.

Every run made by the author using this technique showed either a pronounced "flat" region or a point of inflection in the graph of log H_z/H_o vs. t. Careful examinations of these data, as well as the runs made by Jury, revealed that these anomalous points <u>consistently</u> occured when the temperature of the gold surface had reached -40°F to -35°F. Figure 7 shows two typical sets of runs (numbers 25,26, 27 and 28,) made under duplicate conditions except for the velocity of the air stream. The data for these runs

FIGURE 7
EFFECT OF HYGROMETER TECHNIQUE ON EXPERIMENTAL DATA

Bed length 2"

Velocity - 19.8 cu.ft.per hr.
- o----- Run No. 27
- o——— " " 28
- ●——— " " 32

Velocity - 9.3 cu.ft.per hr.
- o----- Run No. 25
- o—·—· " " 26
- ●——— " " 30

$\frac{H_z}{H_o}$

1.0
0.1
0.01
0.001

0 50 100 150 200 250 300

Time - Minutes

are given in the Appendix.

The new modified technique consisted of first following the old procedure until a surface temperature of -40°F was reached. From here on, the surface was completely cleared of deposit by heating after each reading. After clearing was complete, the temperature was lowered again and adjusted until equilibrium between a new deposit and the air had been reached. The character of the deposit was observed and noted at all times. It was always found to be ice below -40°F, but above was usually water. The humidity was calculated accordingly. The runs shown in Figure 7 were repeated using this technique and the results are plotted on this same Figure as runs 30 and 32. It is seen that the irregularities in the curves were eliminated. All succeeding runs were made in this manner. Further details on these runs are presented below.

The discoveries regarding the nature of these deposits which led to the modified technique of using the hygrometer were very unexpected and very important, not only in obtaining correct results, but also in explaining the queer data previously gathered. It seems likely that when the old technique was used, water often deposited on top of the ice as temperatures in the neighborhood of -40 to -35°F were reached during a run. Since the water was slow to crystallize, the outer layer in contace with air was at the vapor pressure of water rather than ice.

However, crystallization probably occured slowly from below when the water and ice were in contact as additional water deposited on top. The light reflection characteristics of the surface were then due to a shifting combination of ice and water and the readings of current in the photoelectric cell were not a reliable indication of equilibrium (or lack of it) between the air and the deposit. Likewise, the thermocouple readings were not a reliable indication of the temperature of the outer layer of deposit since it would be insulated by a layer of ice. During this state of uncertainty (not realized at the time) the humidity of the air would appear to be relatively constant. After a time, however, the entire deposit probably crystallized, which made the vapor pressure at the surface far too low for equilibrium with the air and it was necessary to raise the temperature rapidly. Thus the humidity of the air appeared to increase suddenly. However, this sort of thing did not occur on every run made by the old technique as some of Jury's runs showed no flats or inflection. (See page 44.) In other words, one cannot rely on the deposition of ice or water, but must make every reading with a freashly cleared surface and actually observe the nature of the deposit.

Apparently, all of the erratic nature of the earlier runs was due to the improper use of the hygrometer rather than to any variation in feed air humidity or in

the regeneration process. A great deal of time and some twenty five runs were spent in tracking down these experimental difficulties. It is felt that the present set-up and technique of operation is quite good and free of serious errors, and that this has been one of the principal contributions of this study toward solution of the general problem. The graphs plotted on Figure 7 show that the reproducibility of the data is good.

Experimental Results:

It was hoped that Jury's data could be used to carry out an analysis of the rate-controlling mechanism as outlined in the section on the theoretical approach. However, it was felt that all runs exhibiting the anomalous behaviour should be rejected as being suspect for the ice-water difficulties just discussed. The remaining runs available for theoretical analysis are summarized below. Readers are referred to Jury's thesis (11) for the original data from these runs.

From the temperatures determined with the hygrometer using the old technique, Jury calculated the values of H_z, using the vapor pressure of ice as obtained from Whipple's empirical equation quoted by Brunt (3) and assuming P = 14.7 psia in equation (36). He then computed H_z/H_o, with H_o also based upon P = 14.7 psia, and then plotted log H_z/H_o vs. t. Since we need only to work with ratios of absolute humidities, it is not necessary to correct the values

of H to the prevailing atmospheric pressure as this correction would cancel. The plots are not reproduced here.

Jury's Data Available for Theoretical Analysis

Diameter of bed = 1.03" in every run.
Humidity of feed air = 1320 x 10^{-6} pounds of water per pound of air.
Desiccant material: Commercial Drierite, screened and reactivated in muffle furnace two hours at 400°F.
Weight of material in bed not determined.

Jury's Run No.	Bed Length Z-inches	Granule Mesh	Air Flow -cu.ft.hr.	Ambient Temp. - °F
3	2	20-24	9.4	70
4	3	4-5	9.4	75
5	4	20-24	9.4	72
6	3	2-2 1/2	9.4	76
7	2	20-24	7.0	73
8	3	20-24	9.4	74
14	3	20-24	9.4	66
19*	2	20-24	9.4	76

* = Reactivation for 4 hours at 450°F.

All of these runs, as well as all made by the author, were essentially isothermal at room temperature. Of these runs, numbers 8 and 14 are duplicates and agree very well. Run number 6 made with 2-2 1/2 mesh material in a bed 1" in diameter is no doubt unreliable because of channeling effects. There is possibly the same objection, though perhaps to a lesser degree, to run number 4 made with 4-5 mesh material. The remaining runs are all but one (No. 7) at the same air flow rate and are with the same granule size. Hence, little could be learned from them about the mechanism except as to whether the individual

runs would fit the solution F, equation (32) or not.

It seemed desirable to make a series of runs at various flow rates of air with all other conditions maintained constant. This set of runs was made by the author with the new regeneration apparatus and the new techniques of using the hygrometer. The material used throughout all came from the same batch of commercial Drierite screened and regenerated in situ by the procedure described on pages 50-54. In some cases the bed was regenerated two or more times and re-run without disturbing. Whenever it was finally emptied, the material was heated at 800°F for several hours to determine the dry weight of desiccant packed into the bed. In every case, the bed and feed air stream were at room temperature. The humidity of the air stream was fixed by adjusting the pressure control to 40 psig.

The following table summarizes the conditions for this set of runs. The detailed data obtained are given in Tables VII through XVI in the Appendix. Figure 8 is a plot of all this data in terms of log H_z/H_o vs. time. In calculating values of H_z/H_o the appropriate vapor pressure of ice or water was used, as determined by actual observation of the nature of the deposit.

Summary of Runs at Various Flow Rates

Bed length = 2.03": bed diameter = 1.06".
Desiccant = 10-12 mesh commercial Drierite,

reactivated *in situ*.
Feed air humidity = 1012 x 10^{-6} pounds water per pound air.

Run Number	Air Flow Rate cu. ft. hr.	Times Regenerated	Weight of Dry Desiccant - gms.
30	9.3	1	30.09
34	14.0	2	29.26
35	14.0	1	29.26
32	19.8	3	30.09
37	24.0	3	30.09
42	29,8	1	....

Runs number 34 and 35 are duplicates and agree fairly well. Runs 30 and 32 have been referred to previously in connection with Figure 7. It is to be noted that the weight of desiccant is the same within 3% in all runs, consequently the porosity of packing must have been the same also. There is over a three-fold variation in air flow rate therefore also in mass velocity since all runs were made on beds of the same diameter.

There are two principal differences between the conditions of Jury's runs cited above and those made by the author: particle size of desiccant, and humidity of feed air. Jury worked mostly with 20-24 mesh granules regenerated in the furnace, the author always with 10-12 mesh regenerated *in situ*. Jury used air saturated at 29 psig and 32°F (frost point + 10.3°F, H_o = 1320 x 10^{-6}), the author air saturated at 40 psig and 32°F (frost point 5.5°F, dew point + 1.0°F, H_o = 1012 x 10^{-6}). In both cases the value of H_o lies below the upper limit for which the linear adsorption isotherm holds, as determined by Jury.

FIGURE 8

EFFECT OF AIR VELOCITY ON BED PERFORMANCE

Bed length 2"

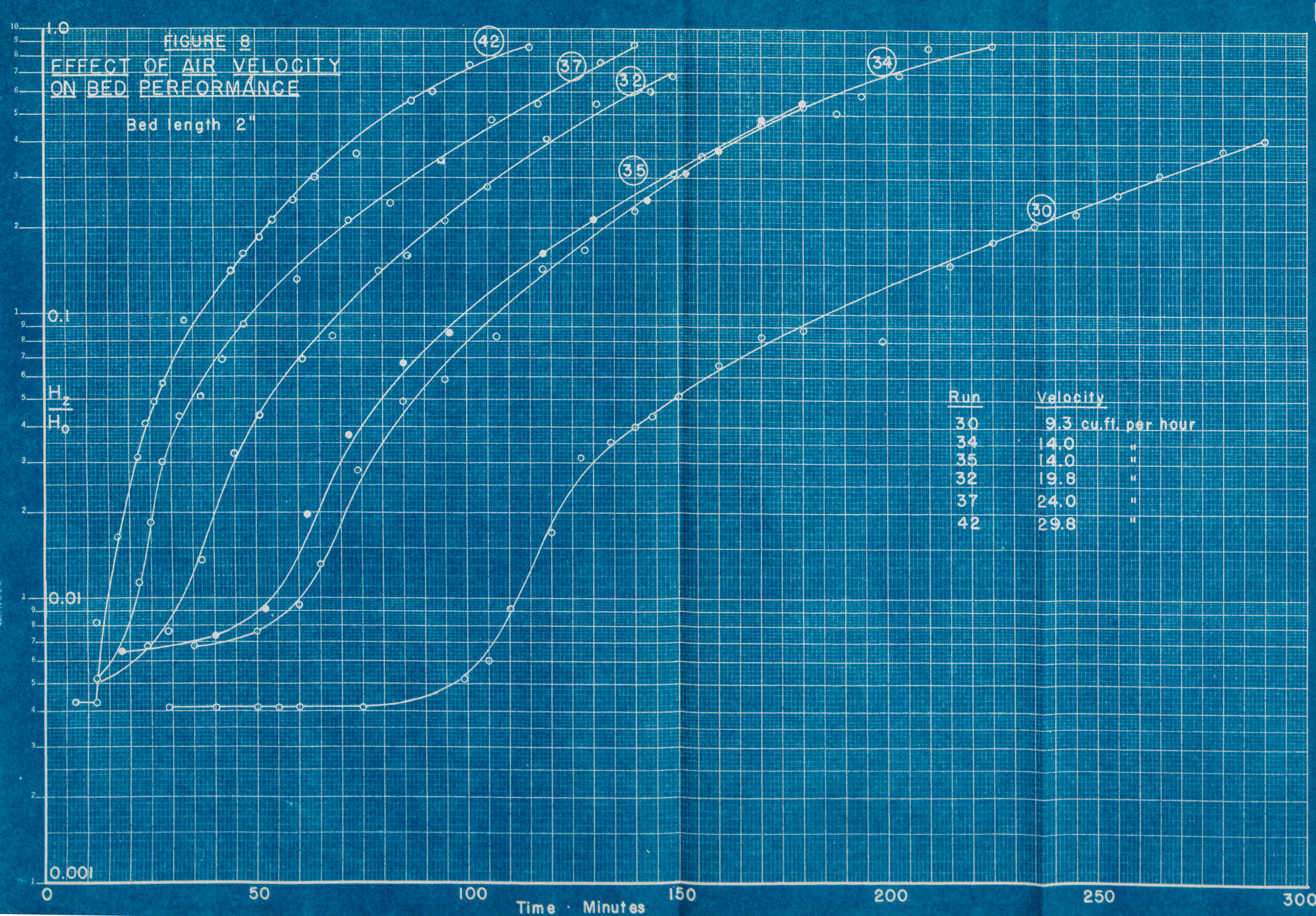

Run	Velocity
30	9.3 cu.ft. per hour
34	14.0 "
35	14.0 "
32	19.8 "
37	24.0 "
42	29.8 "

Analysis of Experimental Data

Vapor Pressure Values

In the calculation of absolute humidity from the temperature readings of the hygrometer, it is important to have reliable data for the vapor pressure of ice and water. Accordingly, a search of the literature was made for such data in order that it might be possible to select and use the best values available.

The following sources of data on the vapor pressure of ice were found:

1) "Thermodynamic Properties of Steam" -- Keenan and Keyes (12). Range: 82°F to -40°F.

2) "Smithsonian Meteorological Tables" -- 5th Edition (17). Range: 0°C to -70°C.

3) "Handbook of Meteorology" -- Berey, Ballay, and Beers (1). Range: 0°C to -40°C.

4) "Physical and Dynamical Meteorology" -- Brunt (3). An empirical equation due to Whipple (20); no range stated.

The first three of these are tables, the fourth an empirical equation which is claimed to represent other data well. Values from all four of these sources were carefully plotted on a large scale for a temperature range from 32°F to -90°F, and the best smooth curve drawn through them. The agreement was excellent over most of the range. Values read from the smoothed curve were used to calculate absolute humidities, using equation (35) for Table V given in the appendix.

Reliable data on the vapor pressure of sub-cooled water at low temperatures were more difficult to find. The following sources were used:

1) "Handbook of Meteorology" - Berry, Ballay, and Beers (1). Range: 0°C to -20°C.

2) "Physical and Dynamical Meteorology" -- Brunt (3). An empirical equation due to Whipple (20); no range stated.

3) Bulletin GEA-4613 - General Electric Co. (6). Range 140°F to -100°F; no source of data stated.

4) Alnor Dew Pointer Instructions - Illinois Testing Laboratories, Inc. (10). A chart, range = 110°F to -100°F; no source of data stated.

All of these data were treated in the same manner as that for ice, described above. The agreement among the various sources, particularly at the lower temperatures, was not quite as good. The calculated humidities are given in Table VI of the Appendix.

It is of interest to note in passing, how the vapor pressure of ice and water compare at the same temperature. Figure 9 shows the ratio of vapor pressures at various temperatures. The ratio (water/ice) rises from 1 at 32°F to 2.0 at -90°F. This clearly indicates the importance of knowing the nature of the hygrometer deposit, as errors of up to 100% in the calculated humidity might be made by using the wrong vapor pressure.

Analysis of Data from Experimental Runs:

FIGURE 9
RATIO - VAPOR PRESSURE OF WATER TO VAPOR PRESSURE OF ICE

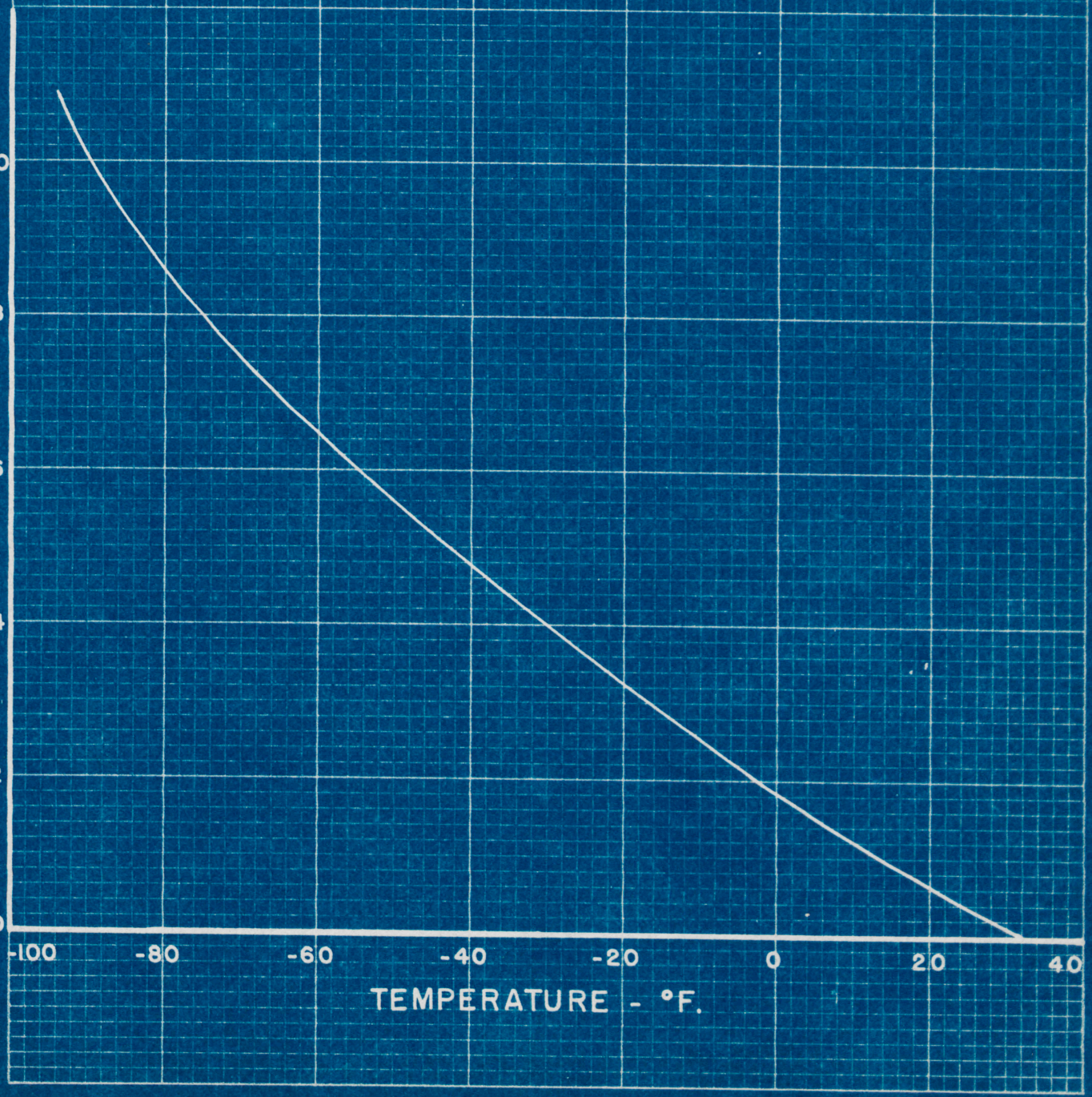

10 x 10 to the inch.

All of the experimental data for H_z vs. t was first prepared in the form of graphs of log H_z/H_o vs. t as mentioned previously. This was done in order that smooth curves might be drawn and used for reading values at any desired point. The construction of these graphs was carried out in accord with the properly calculated H_z values determined by the nature of the deposit. It was necessary for the author to replot Jury's data for the runs listed on page 71 as the graphs presented in his thesis cannot be read with suitable accuracy, due to a lack of sufficient coordinate lines. These plots, however, are not reproduced here.

It was first desired to test all these curves for conformity with the approximate solution, equation (32). This was done in two ways: first by assuming $H_i^* = 0$, and second, by estimating a value for H_i^* from the lowest value of H_z obtained during the initial portion of each run. In both cases, it was necessary to modify somewhat, the testing procedure outlined on page 32.

When H_i^* was taken as zero, step 1 of the procedure was omitted and step 2 became merely the plotting of log H_z/H_o vs. t already mentioned. Step 4 was modified merely in that values of t were read from the smooth curve to correspond with values of H_z/H_o of, say, 0.006, 0.008, 0.01, 0.02, etc. In step 5, of course, the values of Y corresponded to those of H_z/H_o. The remaining steps

were all carried out as stated. Figure 10 shows the plot of Y vs. $\sqrt{t}$ for Jury's runs, and Figure 11 for the author's. On these graphs, the solid circles and solid lines correspond to taking $H_i^* = 0$. The solid curves are drawn through these points.

To determine the effect of correcting H_i^* to some value other than zero, the testing was repeated using as H_i^*/H_o the lowest value of H_z/H_o read from the original plots. Now since

$$F = \frac{H_z - H_i^*}{H_o - H_i^*} + \frac{H_z/H_o - H_i^*/H_o}{1 - H_i^*/H_o}$$

it is possible to work with these ratios in the testing procedure rather than with the absolute humidities themselves. Having selected H_i^*/H_o, a series of values of H_z/H_o to correspond with rounded values of F (as 0.006, 0.008, 0.01, 0.02, etc., were calculated from:

$$H_z/H_o = (1 - H_i^*/H_o)\ F + H_i^*/H_o$$

These values of Hz/H_o were then used to read values of t from the original curves. This procedure replaced the first 4 steps of the testing procedure, and made it unnecessary to construct additional graphs of $\log \frac{H_z - H_i^*}{H_o - H_i^*}$ vs. t. This would have been a waste of effort because of the uncertainty of values for H_i^*. The remainder of the procedure was followed unmodified. The corrected points of Y vs. $\sqrt{t}$ are shown again on Figures 10 and 11 by the open

FIGURE 10
TEST OF JURY'S DATA

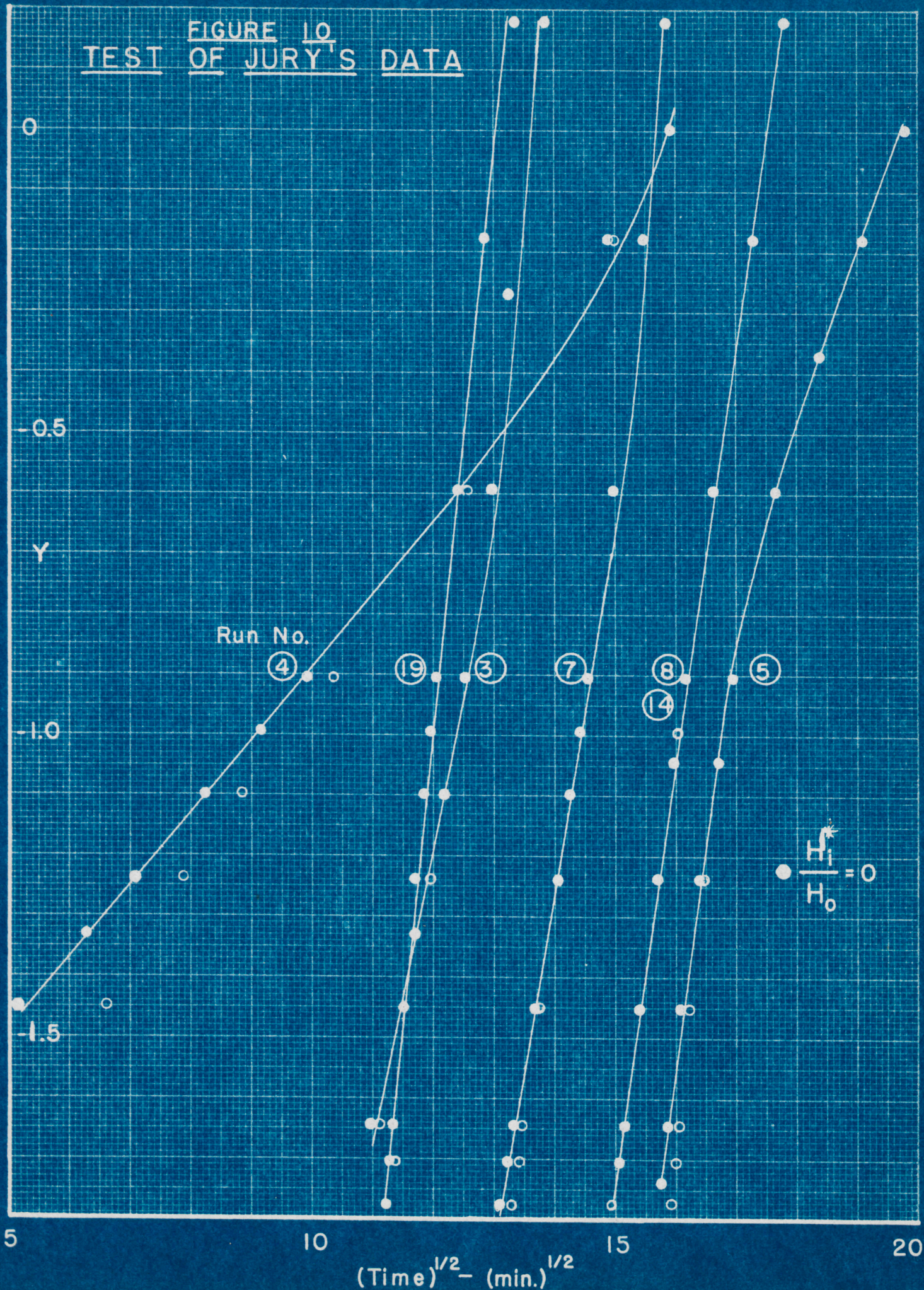

FIGURE 11
TEST OF AUTHOR'S DATA

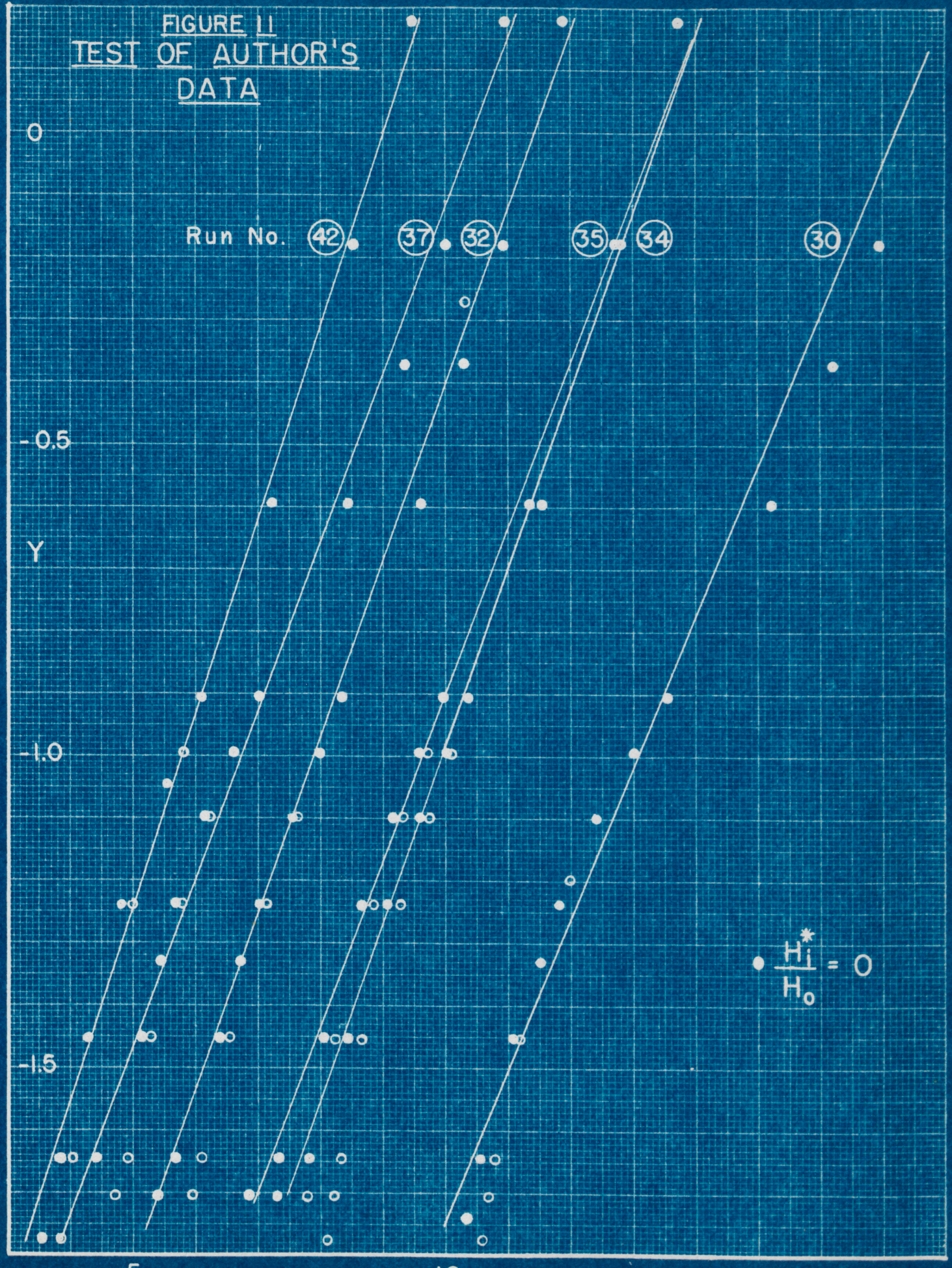

circles. The values of H_i^*/H_o used in each case are tabulated below.

Jury's Data

Run No.	H_i^*/H_o
3	0.0042
4	0.014
5	0.0023
7	0.0032
8	0.0030
14	0.0016
19	0

Author's Data

Run No.	H_i^*/H_o
30	0.00415
32	0.0052
34	0.0070
35	0.0070
37	0.0040
42	0.0043

It is observed that in every case, the corrected points lie to the right and below the solid curves with the gap between them narrowing rapidly as Y approaches -1.0 and being virtually negligible above that. This means that the values of H_i^*/H_o are small enough so that the correction of subtracting them from H_z/H_o is negligible when H_z/H_o is approximately 0.01 or above. The values of H_i^*/H_o used represent the largest that there possibly could have been, and, in fact, the true values might actually have been much smaller than these. The difference between the two sets of points represents the maximum correction. The actual correction, of course, depends upon how much moisture was left in the bed at the end of the regeneration process. Air flowing through the bed cannot possibly be dried below a value in equilibrium with this. Hence, the lowest value to which the air was observed to be dried was taken an approximation to the initial state of the bed. The principal error in doing

this lies in the fact that in some runs, the initial hygrometer readings could not be made soon enough at the start before the H_z values began to rise.

Considering Figure 10, it is seen that three of the runs give good straight line plots of Y vs. $\sqrt{t}$, viz. Jury's number 8, 14, and 19. Runs 8 and 14 are duplicates and coincide on the plot. In all three cases, the correction, which could be made by not taking $H_i^* = 0$, is negligible throughout. Runs number 3, 4, and 7, although plotting as nearly straight in the lower ranges of Y, curve abnormally upward at the higher end. Run number 5 is just the reverse. Runs number 3, 5, and 7, would have much straighter plots in the lower range when a corrected H_i^* is used. Run number 4, however, would become curved in the opposite direction.

In Figure 11, none of the plots, either corrected or uncorrected, would be exact straight lines. They would all curve somewhat downward in the lower range, and upward in the higher range, the curvature being more pronounced when the corrected points are considered. However, in an attempt at smoothing this data, the straight lines have been drawn as an average position about which the curves wind.

From the straight lines drawn on these two graphs, the following values of b and X have been calculated.

Values of the Constants b and X

Jury's Data: Figure 10

Run No.	Position of Graph	b-min.$^{-1}$	X
4	Lower, uncorrected	0.0136	4.25
19	Entire	1.00	169
3	Lower, corrected	0.301	61
7	Lower, corrected	0.306	84
8	Entire	0.467	144
14	Entire	0.467	144
5	Lower, corrected	0.861	273

Author's Data Straight lines - Figure 11

Run No.	b-min.$^{-1}$	X
42	0.096	7.8
37	0.073	8.0
32	0.082	10.6
35	0.072	12.1
34	0.082	14.7
30	0.059	17.3

In the case of the author's data, it is unfortunately true that the values of X, approximate though they may be, are all low enough that some doubt is cast upon the accuracy of using the approximate function F to represent E, the accurate solution. There is no question of this in the case of Jury's data with the exception of Run No. 4, where X = 4.25. All of the author's data were accordingly tested against the Schumann-Furnas chart using the values of X listed above as a first approximation. It was found that by using the nearest integral value for X (except for run 32, where X = 10 gave a better fit than X = 11) a value of b could be found that in all cases gave a rather good fit to the curve on the chart in the range

from H_z/H_o = 0.01 upwards to about 0.40. These values are tabulated:

Author's Data	Fitted to Schumann-Furnas Chart	
Run No.	b-min.$^{-1}$	X
42	0.088	8
37	0.065	8
32	0.069	10
35	0.060	12
34	0.076	15
30	0.053	17

At the upper end of all these runs, there is deviation from the corresponding curve on the Schuman-Furnas chart in the direction of more rapid exhaustion of the bed. This accords with the same observation for all of Jury's runs as interpreted by the Y vs.$\sqrt{t}$ plots. Thus the state of affairs anticipated on page 16 is found to exist, wherein as the bed approaches saturation the internal resistance increases, and the rate of exhaustion increases over that prevailing at a constant value over the first portion of the run. So it is clear that we are dealing with a case of at least one varying resistance, and that no one of the individual kinetic relationships proposed can possibly hold throughout the runs. Consequently, the differential equation (22) cannot describe the behavior of the bed throughout the run.

However, over the first portion of the run conformity with the solution to the differential equation is obtained with the values of the constants b and X as

tabulated above. We may subject these values to certain tests to determine whether this conformity is due to one of the proposed kinetic relationships. For this purpose refer to Table II. With the data available, we may test the effect of mass velocity, particle size, and bed length on b and X.

Effect of Air Flow Rate

The table indicates that if the mass transfer kinetic relationship holds:

$$X \propto \frac{d}{G^n} \quad \text{and} \quad b \propto dG^{1-n}$$

provided the air flow is turbulent so that $n \neq -2$. If either internal diffusion or the shell diffusion kinetic relationship applies

$$X \propto \frac{1}{G} \quad \text{and} \quad b = \text{constant}$$

insofar as mass velocity alone is concerned. To test which, if any, of these proportionalities holds for the present data, it is necessary merely to plot log X vs. log G, and log b vs. log G and determine whether a straight line is obtained, and if so, the value of the slope of the line. Since all experiments were run at the same conditions of temperature and pressure, and in beds of the same diameter, G is directly proportional to the flow rate as measured in cu. ft. per hour. Hence, plots of log X vs. log (cfh) and log b vs. log (cfh) will be satisfactory for the purpose, and values of G need not be computed.

The data available for this test consists of all of the author's runs and numbers 3 and 7 of Jury's runs. The following values were used to construct the log-log plots on Figure 12.

Run No.	Flow Rate-cfh	X	b-min.$^{-1}$
Author's Data			
30	9.3	17	0.053
34	14.0	15	0.076
35	14.0	12	0.060
32	19.8	10	0.069
37	24.0	8	0.065
42	29.8	8	0.088
Jury's Data			
3	9.4	61	0.301
7	7.0	81	0.306

The solid lines represent the best smooth lines which may be drawn through the points. They are all straight within the limits of accuracy of the data. The slopes were measured and found to be as follows:

Plot	Slope	n
Author's X vs. cfh	-0.65	0.65
" b vs. cfh	0.45	0.55
Jury's X vs. cfh	-1.02	1.02
b vs. cfh (not plotted)	0	1

The data from the author's runs conformed to the situation for mass transfer; those from Jury's runs corresponds to an internal process; but include only two points and cannot be accepted as conclusive. On Figure 12 dashed lines have been drawn through the author's data in the positions they would occupy if the proportionalities for internal diffusion

FIGURE 12

TESTS FOR CONTROLLING RESISTANCE

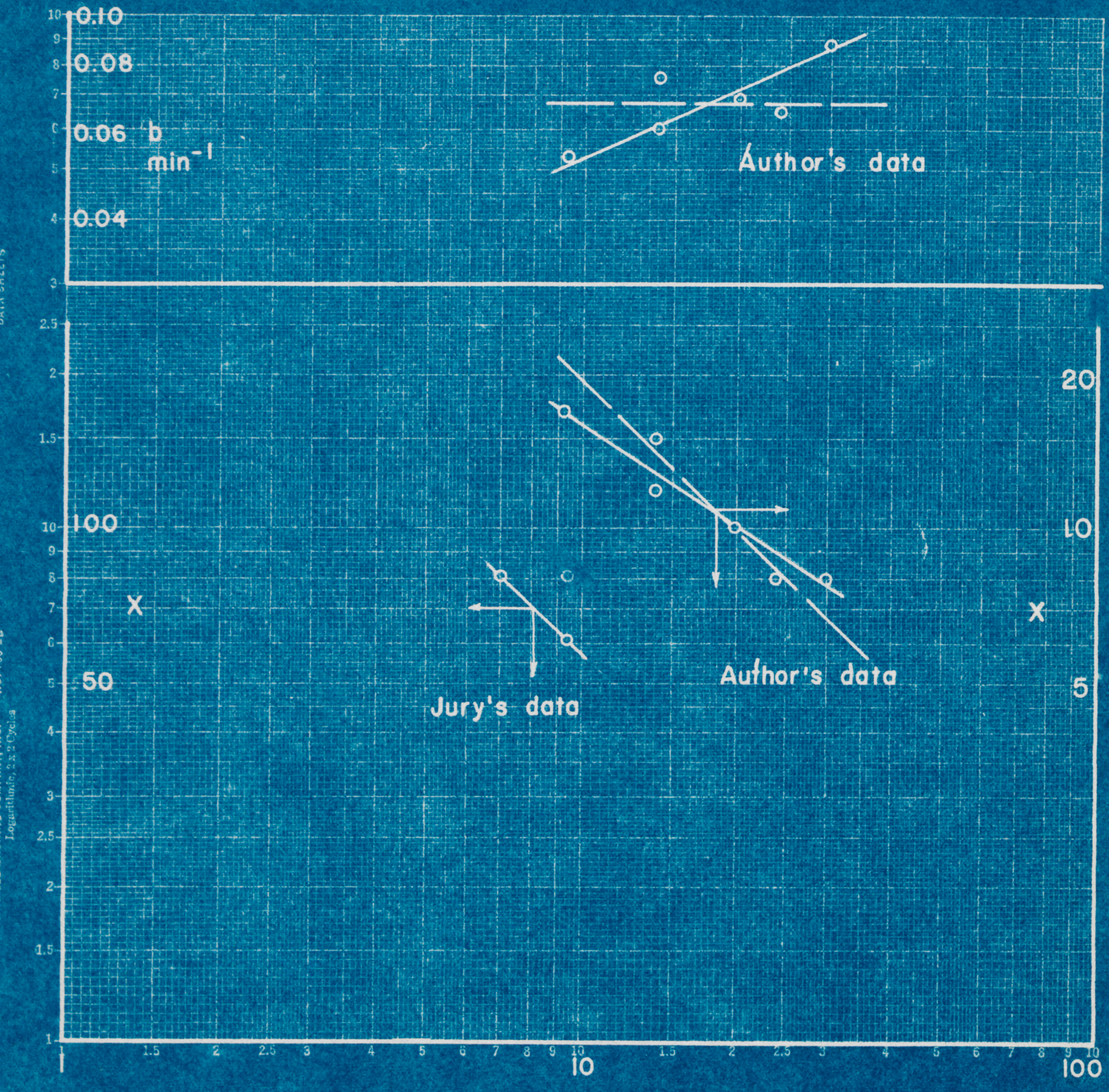

or shell diffusion held. It is evident that such lines do not represent the data. There is no doubt that mass transfer can be distinguished as the rate controlling process during the earlier portion of the runs. The values of n found do not agree exactly with those of Gamson, et al (5,23) but are very closely in the same range. An exact agreement could not be expected, for the data of Gamson, et al were obtained on catalyst pellets of regular shape Here we are dealing with very irregular granules having a relatively large surface area.

The value of n = 1 for Jury's runs, while not conclusive, may be an indication that mass transfer resistance has decreased and become negligible in comparison with internal diffusion for the smaller granules used in his runs. According to equation (8) $K_G \frac{1}{R^n}$ which is in line with this agreement.

Effect of Particle Size

Two tests might be attempted with the data at hand. First, Jury's run number 3 and the author's number 30 were made at virtually the same velocity (9.4 cfh and 9.34 cfh), but with different particle size (20-24 mesh, and 10-12 mesh), and different feed air humidity.

(H_o = 1012 x 10^{-6}, and H_o = 1320 x 10^{-6})

The difference in feed air humidity should have little effect upon the constants, so that the following propor-

tionalities pertaining to granule size might be tested.

$X \propto \frac{d}{R^{1+n}}$ $\quad b \propto \frac{d}{R^{1+n}}$ for mass transfer; $n < 1$

$X \propto \frac{1}{R^2}$ $\quad b \propto \frac{1}{R^2}$ for internal diffusion; $n = 1$.

$X \propto \frac{1}{R}$ $\quad b \propto \frac{1}{R}$ for shell diffusion; $n = o$

The average particle sizes used in these two runs can only be estimated by taking the average of the limiting screen sizes in each case. For Jury's run, 20-24 mesh granules were used, for the author's 10-12 mesh. The ratio of sizes should be 1:2. The values found for the constants were:

Jury's No. 3	Author's No. 30
$X_3 = 61$	$X_{30} = 17$
$b_3 = 0.301$	$b_{30} = 0.053$
$\frac{X_3}{X_{30}} = \frac{61}{17} = 3.59$	$\frac{b_3}{b_{30}} = \frac{0.301}{0.053} = 568$
$(2)^{1+n} = 3.59$	$(2)^{1+n} = 5.68$
$n = 0.84$	$n = 1.5$

The test is not conclusive. The value of $n = 0.84$ obtained from the ratio of X's would correspond to mass transfer, while that of $n = 1.5$ from the ratio of b's is too high for any of the cases.

A similar test may be made by comparing Jury's

runs number 4 and 8. These were made in beds of 3" length, at the same velocity, 9.4 cfh., same humidity $H_o = 1320 \times 10^{-6}$, and with granules 4-5 mesh, and 20-24 mesh respectively. The ratio of particle sizes, based upon the average screen openings is 5.63. The constants are:

Run 4	Run 8
$b_4 = 0.0136$	$b_8 = 0.467$
$X_4 = 4.25$	$X_8 = 144$

Ratios:

$$\frac{X_8}{X_4} = \frac{144}{4.25} = 33.9 \qquad \frac{b_8}{b_4} = \frac{0.467}{0.0136} = 34.4$$

$$(5.63)^{1+n} = 33.9 \qquad (5.63)^{1+n} = 34.4$$

$$n = 1.04 \qquad n = 1.05$$

The values of n conform very closely to the ratio for internal diffusion. But again, the test cannot be accepted as conclusive because of the possibility of channeling being present in run No. 4, in which 4-5 mesh granules (avg. 0.1702) were contained in a bed of 1" diameter. The tests of isolated cases such as these and the velocity ratio test of Jury's runs number 3 and 7 are not of much value because of the danger of experimental errors entering unnoticed and uncompensated.

The only conclusion which may be established here is that we are dealing with a case of combined resistances which do not remain constant. During the beginning of the run mass transfer seems to control, but as the bed approaches saturation, internal resistances increase to the point where

the rate of exhaustion is accelerated beyond that to be expected from the beginning of the run.

Effect of Bed Length

According to Table II, only X should be affected by the length of the bed and then in direct proportion, if all other variables are held constant. Three of Jury's runs may be used to test this point. These were run under identical conditions, save for the bed length. The data are:

Run No.	Bed Length	X	b
3	2"	61	0.301
8.14	3"	144	0.467
5	4"	273	0.861

The ratios of bed length are 1: 1-1/2: 2, but the ratios of X values are 1: 2.36: 4.48, very poor agreement.

It is difficult to determine the reason for this. Since the weight of material in each bed was not obtained by Jury, we cannot be sure that the beds were packed uniformly and tightly. There may have been some motion of the particles or readjustment of position due to the lubricating effect of the flowing stream. Further, there may have been differences introduced by the method and conditions of regeneration. Some indication of this appears by comparing Jury's runs 3, and 19. These were duplicates, except that in the case of run 19, regeneration was carried out at 450°F for 4 hours, whereas for all others, it was two

hours at 400°F. For run 19 the constants obtained were X = 169, b = 1.00, quite a bit different from those of run 3, and also more in line with the ratios mentioned above. A standardized method of regeneration is certainly necessary in all of this work.

Summary and Conclusions

Summary and Conclusions

The theory of the adsorption wave as applied to a bed of desiccant has been critically reviewed. It has been shown that this theory depends upon a kinetic relationship for the rate of moisture pickup. Several such relationships are presented and shown to be based upon implicit assumptions which make them mutually exclusive, a fact not previously appreciated. All of these relationships, however, lead to the same type of differential equation. Both a complicated, rigorous, and a simplified approximate solution to this equation are presented and a graphical method of testing data for conformity to the latter has been devised. The interpretation of such test results has been outlined in a way to make it possible to determine which, if any, of the kinetic relationships is applicable.

The experimental method of obtaining H_z vs. t data has been carefully reviewed and modified. A new apparatus for the regeneration of a bed *in situ* has been built and used. The technique of using the frost-point hygrometer has been modified as a result of the important discovery that super-cooled water droplets could exist in this apparatus at temperatures as low as -40°F. Additional H_z vs. t data on the effect of velocity of air flow have been obtained.

The author's data, together with some of Jury's data, have been subjected to the testing procedure and found to indicate that we are dealing with a case where none of the kinetic relationships proposed will apply throughout the life of the bed. However, during the initial portion of each run, the differential equation is obeyed. Examination of the relationship between air flow rate and the constants X and b indicate that mass transfer is the principal source of resistance during this portion. During the latter portion of the runs the resistance increases appreciably so that the bed exhausts at an increasing rate. This is attributed to an increase in internal resistance to moisture pick-up as the granules approach saturation.

There is some indication that the effect of mass transfer islessened by using smaller granule sizes.

The data clearly show that the conditions of regeneration must be standardized. The appropriate constants obtained from a given run apply not only to the conditions maintained during the run, but to the condition of the granules used.

Literature Cited

1. Berry, F. A., Bollay, E., and Beers, N.R., "Handbook of Meteorology", Table 68, p. 70. McGraw-Hill Book Co., New York, 1945.

2. Brewer, A. W., Cwilong, B., and Dobson, G.M.B., Proceedings of the Physical Society, 60, 52-70,(1948.)

3. Brunt, D. "Physical and Dynamical Meteorology", Second Edition, p. 103, Cambridge University Press, 1939.

4. Frank, P., and von Mises, F., "Die Differential- und Integral- Gleichungen der Mechanik und Physik", p. 420. Rosenberg, New York, 1943.

5. Gamson, B. W., Thodos, G., and Hougen, O.A., Trans. Ameri. Inst. Chem. Engrs., 39, 1 (1943).

6. General Electric Co., Bulletin GEA-4613, "To Determine the Moisture Content of Gases", p. 8, (1947).

7. Heverly, J. R., Trans. Amer. Geophys. Union, 30, 205-10, (1949).

8. Hougen, O.A., and Marshall, W. R., Chemical Engineering Progress, 43, 197-208 (1947)

9. Hougen, O.A., and Watson, K.M., "Chemical Process Principles Charts", pp. 216, 217. John Wiley and Sons, New York, 1947.

10. Illinois Testing Laboratories, Inc., "Alnor Dewpointer Instructions" Fig. 6, 1950.

11. Jury, S. H., "Drying of Gases. The Adsorption Wave in Desiccant Beds", University of Cincinnati Thesis (Ph.D.), 1949.

12. Keenan, J. H., and Keyes, F. G., "Thermodynamics Properties of Steam", Table 5, p. 76; John Wiley and Sons, New York, 1936.

13. Klotz, I. M., Chemical Reviews, 39, 241-268 (1946).

14. Lange, N. F., "Handbook of Chemistry", 1st Edition, Mathematics Section p. 235; Handbook Publishers Inc., Sandusky, Ohio, 1934.

15. Marshall, W. R., and Pigford, R. L., "The Application of Differential Equations to Chemical Engineering Problems", pp. 163-170; University of Delaware, Newark, Delaware, 1947.

16. Schaeffer, V., General Electric Co., private communication (1947) quoted by Suomi (*18*).

17. Smithsonian Meteorological Tables, Fifth Edition, Table 76, pg. 169, Smithsonian Institute, Washington D.C., 1931.

18. Suomi, V. E., Proc. of the Instrument Society of America, 2, 36-40 (1948).

19. Wheat, T. C., "Mass Transfer in Beds of Chemical Desiccants", University of Cincinnati Thesis (M.S.), 1948.

20. Whipple, Monthly Weather Review, pg. 131 (1927).

21. Wicke, E., Kolloid Z., 86, 167-186, 296-313 (1939).

22. Wicke, E., ibid, 93, 129-157 (1940).

23. Wilke, C. R., and Hougen, O.A., Trans. Ameri. Inst. Chem. Engrs., 41, 445 (1945).

APPENDIX

Table IV

Calibration Data for Thermocouple in Frost-Point Hygrometer

°F	0	1	2	3	4	5	6	7	8	9
+30	.04	.02	0							
+20	.25	.23	.21	.19	.17	.15	.13	.10	.08	.06
+10	.46	.44	.42	.40	.38	.36	.34	.31	.29	.27
+ 0	.67	.65	.63	.60	.58	.56	.54	.52	.50	.48
- 0	.67	.69	.71	.73	.75	.77	.79	.81	.83	.85
-10	.87	.89	.91	.93	.95	.97	.99	1.01	1.03	1.05
-20	1.07	1.09	1.11	1.13	1.15	1.17	1.19	1.21	1.23	1.25
-30	1.27	1.29	1.31	1.33	1.35	1.37	1.39	1.41	1.43	1.45
-40	1.47	1.48	1.50	1.52	1.54	1.56	1.58	1.60	1.62	1.64
-50	1.65	1.67	1.69	1.71	1.73	1.75	1.77	1.79	1.80	1.82
-60	1.84	1.86	1.88	1.90	1.92	1.93	1.95	1.97	1.99	2.01
-70	2.02	2.04	2.06	2.08	2.10	2.12	2.14	2.15	2.17	2.19
-80	2.21	2.23	2.25	2.26	2.28	2.30	2.32	2.34	2.35	2.37
-90	2.39	2.41	2.42	2.44	2.46	2.48	2.49	2.51	2.53	2.55
-100	2.56	2.58	2.60	2.62	2.63	2.65	2.67	2.68	2.70	2.72
-110	2.73	2.75	2.77	2.78	2.80					

Table V

ABSOLUTE HUMIDITY OF AIR IN EQUILIBRIUM WITH ICE AT VARIOUS TEMPERATURES AND 14.7 psi PRESSURE

Absolute humidity - parts per million ($H \times 10^6$)
Temperature - °F

°F.	0	1	2	3	4	5	6	7	8	9
30	3430		3760							
20	2140		2370		2600		2830		3120	
10	1310	1390	1470		1610		1770		1930	
0	783	826	871	920	970	1012	1070	1125	1180	1245
-0	783	738	709	672	640	602	572	540	509	483
-10	459	435	411	390	368	348	328	311	293	276
-20	261	246	235	221	209	196	184	174	164	154
-30	147	139	134	122	115	107	101	94.3	88.8	83.7
-40	78.9	74.5	70.2	65.1	61.0	57.1	53.5	49.6	46.8	44.1
-50	41.7	39.1	36.3	33.8	31.6	29.2	27.4	25.4	24.1	22.5
-60	2.12	19.9	18.6	17.3	15.9	14.9	13.8	12.8	11.9	11.0
-70	10.2	9.50	8.88	8.25	7.71	7.14	6.58	6.09	5.65	5.22
-80	4.84	4.50	4.15	3.84	3.53	3.27	3.02	2.76	2.56	2.37
-90	2.19	2.02	1.85	1.70	1.55					

Table VI

ABSOLUTE HUMIDITY OF AIR IN EQUILIBRIUM WITH SUB-COOLED WATER AT VARIOUS TEMPERATURES AND 14.7 psi PRESSURE

Absolute humidity - parts per million ($H \times 10^6$)
Temperature - °F

°F.	0	1	2	3	4	5	6	7	8	9
30	3470		3760							
20	2290		2480		2710		2940		3190	
10	1470	1540	1610		1760		1920		2100	
0	933	977	1030	1075	1120	1165	1230	1285	1340	1405
-0	933	890	846	808	771	737	703	669	634	606
-10	578	550	522	497	472	450	426	405	385	369
-20	347	330	313	296	281	267	253	239	226	215
-30	204	190	183	174	164	155	146	139	130	124
-40	117	110	104	98.2	92.5	87.5	82.0	79.3	72.7	69.5
-50	64.6	60.9	57.2	54.0	50.9	47.8	44.7	41.9	39.1	36.9
-60	34.8	32.7	30.6	28.7	26.8	25.1	23.4	21.8	20.5	19.3
-70	18.0	16.9	15.8	14.8	13.8	12.9	12.0	11.2	10.4	9.79
-80	9.19	8.54	7.89	7.33	6.77	6.28	5.78	5.37	4.97	4.66
-90	4.35	4.07	3.79	3.51	3.24					

Table VII

Experimental Data for Run No. 25
February 8, 1950

Description of Run: Flow rate of air 9.3 cu. ft. per hr.
Bed length 2"
Bed diameter 1"
Granule size - 10-12 mesh Drierite
Previous use: None
Pressure of air supply 40 psig.
$H_o = 1012 \times 10^{-6}$ (basis for H_z/H_o)

Elapsed Time - min.	Frost Point °F.	H_z/H_o	Deposit* Assumed	Elapsed Time - min.	Frost Point °F.	H_z/H_o	Deposit* Assumed
	Bed						
0							
22	-86.5	0.00292	ice	145	-48.5	0.0449	ice
27	-88.0	0.00253	ice	155	-45.0	0.0565	ice
35	-88.5	0.00237	ice	162	-42.5	0.0669	ice
62	-88.5	0.00237	ice	170	-40.0	0.0780	ice
75	-79.5	0.0050	ice	178	-38.0	0.0878	ice
85	-75.0	0.00705	ice	190	-34.0	0.114	ice
95	-75.0	0.00705	ice	201	-32.5	0.127	ice
109	-70.0	0.0101	ice	210	-31.0	0.137	ice
115	-66.5	0.0131	ice	224	-29.0	0.152	ice
122	-61.0	0.0196	ice	237	-26.5	0.177	ice
128	-57.0	0.0251	ice	245	-25.0	0.194	ice
135	-54.5	0.0304	ice	251	-23.0	0.218	ice
140	-51.0	0.0386	ice	257	-20.5	0.251	ice
					Feed Air		
					+5		ice

*Using old hygrometer technique

Table VIII

Experimental Data for Run No. 26
February 14, 1950

Description of Run: Flow rate of air 9.3 cu. ft. per hr.
Bed length 2"
Bed diameter 1"
Granule size - 10-12 mesh Drierite
Previous use: In run No. 25
Pressure of air supply 40 psig.
H_o = 1012 x 10^{-6} (basis for H_z/H_o)

Elapsed Time - min.	Frost Point °F.	H_z/H_o	Deposit* Assumed	Elapsed Time - min.	Frost Point °F.	H_z/H_o	Deposit* Assumed
	Feed Air +5		ice				
	Bed						
0							
10	-72	0.00878	ice	186	-36.5	.0965	ice
26	-79.5	0.00494	ice	198	-34	.1135	ice
28	-86	0.00296	ice	210	-33	.121	ice
30	-88.5	..0025	ice	232	-30	.145	ice
34	-89	.00237	ice	240	-28	.162	ice
37	-89	.00237	ice	247	-26	.182	ice
54	-89	.00237	ice	252	-24	.207	ice
61	-83.5	.00360	ice	259	-23	.219	ice
64	-80.5	.00463	ice	262	-21.5	.237	ice
70	-77.5	.00573	ice	272	-19	.276	ice
87	-77	.00608	ice	281	-16.5	.315	ice
96	-74	.00762	ice	287	-14	.363	ice
104	-71	.00938	ice	292	-13	.389	ice
112	-65	.0147	ice	297	-11	.439	ice
118	-62	.0187	ice	304	-9	.478	ice
124	-59	.0222	ice	311	-8	.503	ice
134	-53.5	.0323	ice	316	-6.5	.551	ice
140	-50	.0414	ice	321	-5	.595	ice
151	-46	.0528	ice	324	-4	.632	ice
158	-44	.0602	ice	331	-2.5	.682	ice
164	-42	.0693	ice	336	-1.5	.715	ice
170	-40	.0780	ice	340	-1	.730	ice
178	-37.5	.0903	ice				
					Feed Air +5	1	ice

Data on Weight of Desiccant; Runs 25 and 26

Crucible plus desiccant after run 26	79.4135	gm
Tare weight of crucible	48.2319	
Weight of wet desiccant after run 26	31.1816	
Crubible plus desiccant after heating	77.8607	
Tare	48.2319	
Weight of dry desiccant	29.6288	
Weight of water in desiccant	1.5528	
% of water (dry basis)	5.24	

*Using old hygrometer technique

Table IX

Experimental Data for Run No. 27
February 16, 1950

Description of Run: Flow rate of air: 19.8 cu.ft. per hr.
Bed length 2"
Bed diameter 1"
Granule size 10 -12 mesh Drierite
Previous use: None
Pressure of air supply 40 psig.
H_o 1012 x 10^{-6} (basis for H_z/H_o)

Elapsed Time - min.	Frost Point °F	$\frac{H_z}{H_o}$	Deposit* Assumed	Elapsed Time - min.	Frost Point °F	$\frac{H_z}{H_o}$	Deposit* Assumed
Feed Air	+5	1	ice				
Bed							
0							
13	-85	0.0032	ice	116	-17.5	0.299	ice
25	-84	0.0036	ice	121	-15	0.344	ice
32	-79.5	0.0050	ice	128	-11.5	0.418	ice
38	-60	0.0212	ice	134	-8 .5	0.490	ice
45	-55	0.0297	ice	140	-5 .5	0.580	ice
50	-52	0.0359	ice	145	-3 .5	0.649	ice
56	-46	0.0529	ice	155	-2 .5	0.682	ice
66	-39.5	0.0805	ice	160	-1	0.730	ice
78	-34	0.114	ice	170	+2	0.861	ice
87	-31.5	0.135	ice	180	+2 .5	0.886	
95	-27	0.172	ice	193	+3	0.910	
100	-24.5	0.200	ice	198	+4 .5	0.980	ice
106	-21.5	0.237	ice	Feed Air	+5	1	ice
111	-19.5	0.265	ice				

*Using old hygrometer technique.

Table X

Experimental Data for Run No. 28
February 21, 1950

Description of Run: Flow rate of air 19.8 cu. ft. per hr.
Bed length 2"
Bed diameter 1"
Granule size 10-12 mesh Drierite
Previous use: In run No. 27
Pressure of air supply 40 psig.
$H_o = 1012 \times 10^{-6}$ (basis for H_z/H_o)

Elapsed Time - min.	Frost Point °F.	H_z/H_o	Deposit* Assumed	Elapsed Time - min.	Frost Point °F	H_z/H_o	Deposit* Assumed
	Feed Air +1.5		water				
	Bed						
0							
9	-80	0.00480	ice	120	-14	0.364	ice
15	-79.5	0.0050	ice	125	-11	0.431	ice
20	-79	0.00517	ice	131	-9	0.477	ice
25	-77	0.00603	ice	138	-5.5	0.581	ice
32	-73	0.00816	ice	147	-3.5	0.650	ice
36	-67.5	0.0123	ice	152	-1.5	0.716	ice
40	-56.5	0.0262	ice	157	+ .5	0.792	ice
47	-52.5	0.0346	ice	163	+1.0	0.817	ice
55	-47.5	0.0478	ice	169	+2.5	0.887	ice
61	-44.5	0.0585	ice	177	+3	0.911	ice
67	-42.5	0.0669	ice	185	+4	0.960	ice
75	-38	0.0880	ice				
82	-34.5	0.110	ice		Feed Air +5		
87	-31	0.137	ice			1	ice
92	-29	0.153	ice				
99	-25.5	0.188	ice				
106	-22	0.233	ice				
111	-18.5	0.281	ice				
115	-16.5	0.316	ice				

Data on Weight of Desiccant; Runs 27 and 28

Crucible plus desiccant after run 28	79.8601	gm
Tare weight of crucible	48.2350	
Weight of wet desiccant after run 28	31.6251	
Crucible plus desiccant after heating	78.3959	
Tare	48.2350	
Weight of dry desiccant	30.1609	
Weight of water in desiccant	1.4642	
% of water (dry basis)	4.86	

*Using old hygrometer technique

Table XI

Experimental Data for Run No. 30
March 8, 1950

Description of Run: Flow rate of air 9.3 cu.ft. per hr.
Bed length 2"
Bed diameter 1"
Granule size 10-12 mesh Drierite
Previous use: None
Pressure of air supply 40 psig.
$H_o = 1012 \times 10^{-6}$ (basis for H_z/H_o)

Elapsed Time - min.	Frost Point °F.	H_z/H_o	Deposit* Observed	Elapsed Time - min.	Frost Point °F.	H_z/H_o	Deposit* Observed
	Bed						
0							
19	-85	0.00324	ice	144	-49	0.0435	ice
29	-82	0.0041	ice	150	-46.5	0.0510	ice
40	-82	0.0041	ice	160	-42.5	0.0659	ice
50	-82	0.0041	ice	170	-39.0	0.0827	ice
55	-82	0.0041	ice	180	-38.0	.0876	ice
60	-82	0.0041	ice	199	-46.0	.0806	water
75	-82	0.0041	ice	215	-35.5	.148	water
99	-79	0.00515	ice	225	-32.5	.180	water
105	-77	0.00601	ice	235	-30.0	.204	water
110	-71.5	0.0091	ice	245	-28.0	.224	water
120	-63	0.0170	ice	255	-25.0	.265	water
127	-54	0.0312	ice	265	-22.0	.311	water
134	-52.5	0.0352	ice	280	-18	.379	water
140	-50.5	0.0399	ice	290	-16.5	.408	water

*Using modified hygrometer technique.

Table XII

Experimental Data for Run No. 32
March 15, 1950

Description of Run: Flow rate of air 19.8 cu. ft. per hr.
Bed length 2"
Bed diameter 1"
Granule size 10-12 mesh Drierite
Previous use: In runs Nos. 30, 31.
Pressure of air supply 40 psig.
H_o = 1012 x 10^{-6} (basis for H_z/H_o)

Elapsed Time - min.	Frost Point °F	H_z/H_o	Deposit* Observed
	Bed		
0			
12	-79	0.00515	ice
24	-75.5	0.00677	ice
29	-74	0.00763	ice
37	-66	0.0136	ice
45	-53.5	0.0323	ice
51	-49	0.0435	ice
61	-42	0.0693	ice
68	-39	0.0827	ice
79	-36.5	0.141	water
86	-34.5	0.158	water
95	-29	0.212	water
105	-24	0.278	water
119	-16.5	0.410	water
131	-11	0.543	water
144	-9	0.600	water
149	-6.5	0.678	water
	Feed Air		
	+1		water

Data on Weight of Desiccant; Runs 30 and 32

Crucible plus desiccant after run 32	79.8923 gm.
Tare Weight of crucible	48.2345
Weight of wet desiccant after run 32	31.6578
Crucible plus desiccant after heating	78.3196
Tare	48.2345
Weight of dry desiccant	30.0851
Weight of water in desiccant	1.5727
% of water (dry basis	5.22

*Using modified hygrometer technique

Table XIII

Experimental Data for Run No. 34
March 20, 1950

Description of Run: Flow rate of air 14.0 cu. ft. per hr.
Bed length 2"
Bed diameter 1"
Granule size 10-12 mesh Drierite
Previous use: In run No. 33
Pressure of air supply 40 psig.
$H_o = 1012 \times 10^{-6}$ (basis for H_z/H_o)

Elapsed Time - min.	Frost Point °F.	H_z/H_o	Deposit* Observed
	Bed		
0			
15	-69	0.0109	ice
27	-72	0.00878	ice
35	-75.5	0.00677	ice
50	-74	0.00762	ice
60	-71	0.0094	ice
65	-66.5	0.0131	ice
74	-55.5	0.0280	ice
85	-47	0.0490	ice
95	-44.5	0.0584	ice
107	-39	0.0827	ice
118	-36	0.144	water
128	-33.5	0.167	water
140	-27.5	0.229	water
149	-22	0.310	water
156	-19.5	0.354	water
170	-14.5	0.456	water
180	-11.5	0.530	water
188	-12.5	0.503	water
194	-9.5	0.585	water
203	-6	0.695	water
210	-1.5	0.858	water
225	-1	0.880	water
	Feed Air		
	+1.5		water

Data on Weight of Desiccant; Runs 33 and 34

Crucible plus desiccant after runs 33 and 34	79.0875
Tare weight of crucible	48.2326
Weight of wet desiccant after runs 33 and 34	30.8549
Crucible plus desiccant after heating	77.4947
Tare	48.2326
Weight of dry desiccant	29.2621
Weight of water in desiccant	1.5928
% of water (dry basis)	5.44

*Using modified hygrometer technique

Table XIV

Experimental Data for Run No. 35
March 24, 1950

Description of Run: Flow rate of air 14.0 cu.ft. per hr.
Bed length 2"
Bed diameter 1"
Granule size 10-12 mesh Drierite
Previous use: None
Pressure of air supply 40 psig.
$H_o = 1012 \times 10^{-6}$ (basis for H_z/H_o)

Elapsed Time - min.	Frost Point °F.	H_z/H_o	Deposit* Observed
	Feed Air		
	+0.5		water
	Bed		
0			
18	-76	0.00649	ice
23	-73.5	0.00788	ice
40	-74.5	0.00733	ice
52	-71.5	0.00909	ice
62	-61	0.0197	ice
72	-51.5	0.0373	ice
85	-42.5	0.0670	ice
96	-38.5	0.0852	ice
118	-34	0.162	water
130	-29	.213	water
143	-26	0.250	water
152	-22	0.309	water
160	-18.5	0.373	water
170	-13.5	0.478	
180	-11.5	0.530	

*Using modified hygrometer technique.

Table XV

Experimental Data for Run No. 37
March 29, 1950

Description of Run: Flow rate of air 24.0 cu.ft. per hr.
Bed length 2"
Bed diameter 1"
Granule size 10-12 mesh Drierite
Previous use: In runs Nos. 35, 36.
Pressure of air supply 40 psig.
$H_o = 1012 \times 10^{-6}$ (basis for H_z/H_o)

Elapsed Time - min.	Frost Point °F.	H_z/H_o	Deposit* Observed
	Feed Air		
	+1		water
	Bed		
0			
12	-73	0.00815	ice
22	-68.5	0.0113	ice
25	-62	0.0184	ice
28	-54.5	0.0301	ice
32	-49	0.0436	ice
37	-46.5	0.051	ice
42	-42	0.0693	ice
47	-37.5	0.0905	ice
60	-32	0.132	ice
72	-29	0.212	water
82	-21	0.243	ice
94	-15	0.344	ice
106	-9	0.478	ice
117	-11	0.543	water
132	-4	0.762	water
140	-1.5	0.858	water
	Feed Air		
	+1		water

Data on Weight of Desiccant;

Crucible plus desiccant after runs 35, 36, 37	78.8657
Tare weight of crucible	48.2267
Weight of wet desiccant after runs 35, 36, 37	30.6390
Crucible plus desiccant after heating	77.3252
Tare	48.2267
Weight of dry desiccant	29.0985
Weight of water in desiccant	1.5405
% of water (dry basis)	5.31

*Using modified hygrometer technique

Table XVI

Experimental Data for Run No. 42
April 14, 1950

Description of Run: Flow rate of air 29.8 cu.ft. per hr.
Bed length 2"
Bed diameter 1"
Granule size 10-12 mesh Drierite
Previous use: None
Pressure of air supply 40 psig.
H_o = 1012 x 10^{-6} (basis for H_z/H_o)

Elapsed Time - min.	Frost Point °F.	H_z/H_o	Deposit* Observed
	Feed Air +1.5		water
	Bed		
0			
7	-81.5	0.00428	ice
12	-81.5	0.00428	ice
17	-63.5	0.0164	ice
22	-54	0.0312	ice
24	-50	0.0412	ice
26	-47	0.0490	ice
28	-45	0.0565	ice
33	-43.5	0.0943	water
44	-36.5	0.141	water
47	-34	0.162	water
51	-31.5	0.184	water
54	-29	0.213	water
59	-26	0.250	water
64	-22.5	0.301	water
87	-10.5	0.557	water
92	-9	0.600	water
101	-4.5	0.745	water
115	-1.5	0.858	water

*Using modified hygrometer technique.